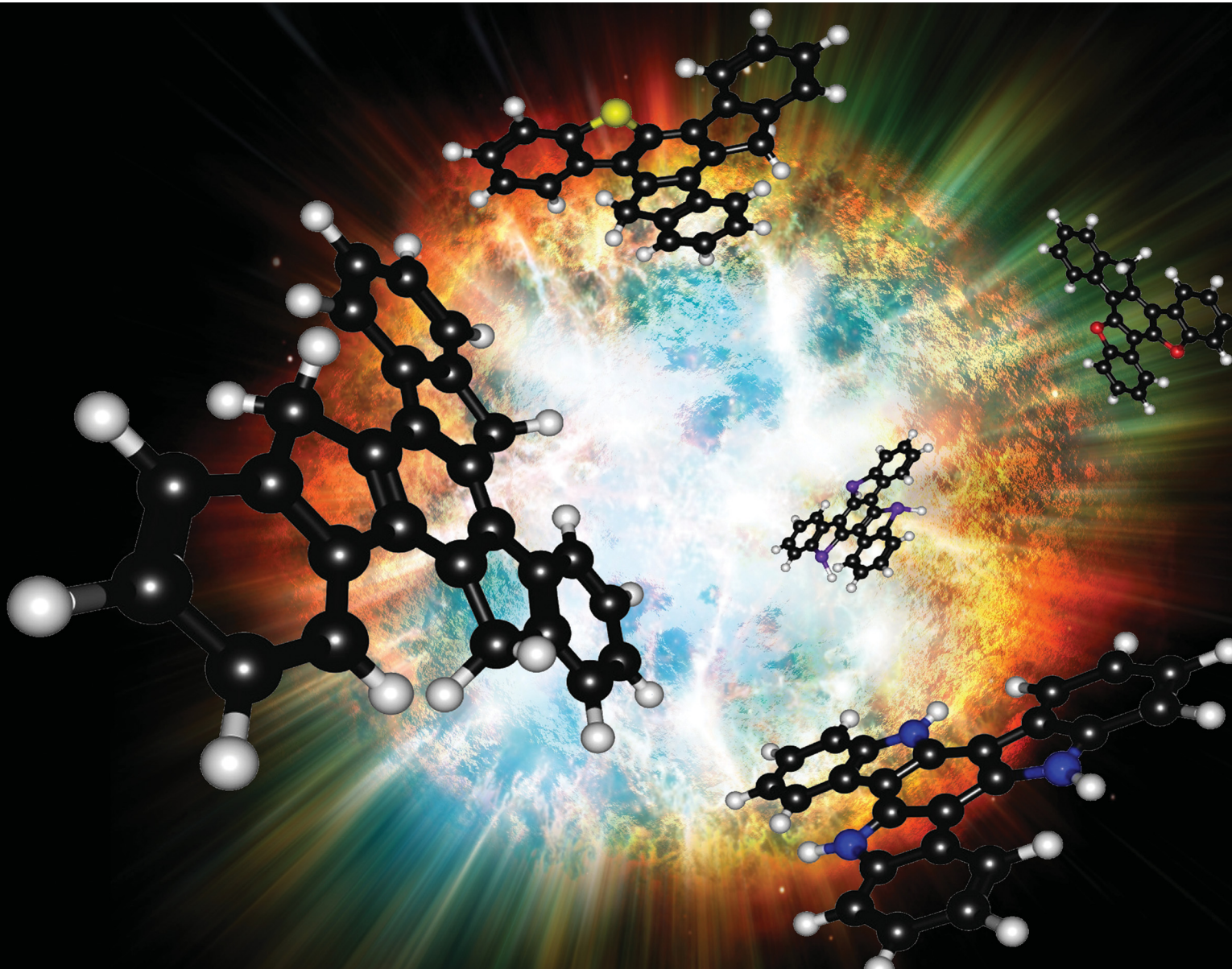


# NJC

New Journal of Chemistry  
rsc.li/njc

A journal for new directions in chemistry



ISSN 1144-0546

**PERSPECTIVE**

Krzysztof Górski, Justyna Mech-Piskorz and  
Marek Pietraszkiewicz  
From truxenes to heterotruxenes: playing with  
heteroatoms and the symmetry of molecules



Cite this: *New J. Chem.*, 2022, **46**, 8939

Received 17th February 2022,  
Accepted 22nd March 2022

DOI: 10.1039/d2nj00816e

rsc.li/njc

# From truxenes to heterotruxenes: playing with heteroatoms and the symmetry of molecules

Krzysztof Górski,<sup>a</sup> Justyna Mech-Piskorz<sup>b</sup> and Marek Pietraszkiewicz<sup>b</sup>

The truxene molecule is more versatile and widespread than ever imagined. At the end of the last century, this star-shaped structure was recognized mostly in liquid crystals. However, the development of optoelectronics resulted in a revolution in truxenes. Stable, fast, easily processed and cheap optoelectronic devices are desirable in many areas of industry and science. Consequently, the contribution of truxenes to these fields is manifold, ranging from D–A emitters, semiconductors, and complexes to sensors. They attract attention because of their relatively low mass and expanded  $\pi$ -electron system. Symmetric molecules give rise to dendrimers, bowl-shape molecules and fullerenes. Further advantages are shown by the recently discovered non-symmetric truxenes obtained *via* one- or two-heteroatom displacement. Thus, the chemistry of new heteroaromatic compounds has been expanded.

## 1. Introduction

Truxene is a  $C_{3h}$  aromatic hydrocarbon possessing seven fused rings, specifically, three five-membered and four six-membered rings, as shown in Fig. 1. Nowadays, this name also refers to its heteroanalogues. Most (hetero)truxenes are cyclotrimerization products of commercially available ketones and oxindoles.

To obtain mono- and diheterotruxenes,  $6\pi$ -electrocyclization is required. The latter requires the synthesis of specific substrates because they are not commercially available. Truxenes has attracted vast interest, similar to other polycyclic aromatics, in the last few years due to the growing demand for organic emitters and semiconductors. Accordingly, scientific efforts are focused on the photostability of materials, purity of their colours, and increasing their charge carrier mobility. Easy processing is also an essential factor. This trend includes truxenes, as evidenced by numerous review papers.<sup>1–5</sup> The typical features of truxenes is their significant thermal and

<sup>a</sup> Institute of Organic Chemistry Polish Academy of Sciences, Kasprzaka 44/52 01-224 Warszawa, Poland. E-mail: kgorski@icho.edu.pl

<sup>b</sup> Institute of Physical Chemistry Polish Academy of Sciences, Kasprzaka 44/52 01-224 Warszawa, Poland. E-mail: jmech@ichf.edu.pl



**Krzysztof Górski**

research interests are focused on the synthesis and physicochemistry of (hetero)aromatic functional dyes.

*Dr Krzysztof Górski received his MSc from Warsaw University in 2012 under the supervision of Professor Marek Pietraszkiewicz and Professor Andrzej Kudelski. He continued his research on heterotruxenes at the Institute of Physical Chemistry of the Polish Academy of Sciences, where he obtained his PhD in 2020 under the supervision of Professor Marek Pietraszkiewicz. Currently, he is a Postdoctoral Researcher in Prof. Daniel Gryko's group. His*



**Justyna Mech-Piskorz**

*She started her own project at the Institute of Physical Chemistry PAS in 2015 concerning the physicochemical aspects of hybrid materials. Currently, she is working on non-linear effects in truxenes and its hybrids.*

*Dr Justyna Mech-Piskorz was born in Bochnia (Poland). She graduated with her MSc Eng. from Jagiellonian University, specializing in photonics and nanotechnology and supervised by Dr Jerzy Zachorowicz. During her PhD studies, she participated in interdisciplinary studies involving chemistry and solid state physics. She graduated with a PhD from AGH University of Science and Technology, supervised by Prof. Konrad*



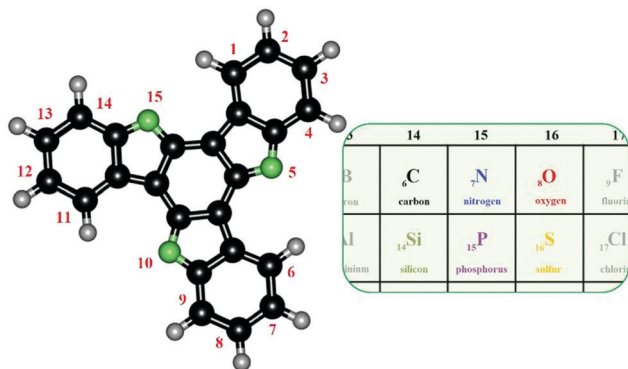


Fig. 1 Possible structures of (hetero)truxenes.

photostability. Truxenes and their heteroanalogues can be utilized in OLEDs,<sup>6–9</sup> OFETs,<sup>10–12</sup> DSSCs,<sup>13–15</sup> NLO,<sup>16–19</sup> sensors,<sup>20,21</sup> gases and small molecule storage<sup>22–24</sup> materials, and many more. The enormous diversity of truxenes is due to the unprecedented possibilities for their functionalization. Their modification can be realized on two levels. The first level is individual molecule derivatization, and the second level is building structured materials from the bottom up. In this manner, materials with designed physicochemical properties and structures can be obtained. Furthermore, heteroatom displacement offers the unique possibility of electronic structure tuning.

One example is 5,10,15-triazatruxene derivatives, which are characterized by a high-lying HOMO of  $-5.1$  eV and exhibit good hole mobility of  $8.9 \times 10^{-4} \text{ cm}^2 \text{ V}^{-1} \text{ s}^{-1}$ .<sup>25</sup> Fig. 1 presents the various configurations of heteroatom(s) insertion. Truxenes, due to their specific structure, can be polyradicals.<sup>26</sup> They are utilized to synthesize strained aromatic moieties,<sup>27</sup> including



Marek Pietraszkiewicz

Prof. Marek Pietraszkiewicz was born in Warsaw (Poland). He obtained his PhD at the Institute of Organic Chemistry, Polish Academy of Sciences, in 1978, with Prof. Osman Achmatowicz as his supervisor. He was a Post-Doc Researcher at Orlean University, supervised by Prof. Pierre Sinay, working on the total synthesis of cerulenin antibiotics. He held a second Post-Doc position at University Louis Pasteur, Strasbourg, France, supervised by

Prof. Jean-Marie Lehn, working on photoluminescent lanthanide complexes. He obtained his DSci (habilitation) at the Institute of Physical Chemistry, Polish Academy of Sciences. His scientific research interests include organic synthesis, supramolecular chemistry, lanthanide photoluminescent complexes, and materials for organic electronics. He is the founder and chairman of the Polish and Global Supramolecular Chemistry Networks.

fullerenes,<sup>28</sup> chiral molecules,<sup>29,30</sup> and supramolecular units.<sup>31,32</sup> The main goal of this review is to present the structure-electronic relationship of truxenes. This information can be beneficial for the appropriate design of truxene-like structures. In the present review, truxenes are systematized in terms of their symmetry (presence or absence of a triple-axis of symmetry). Then, in each of these groups, the different heteroatoms are distinguished.

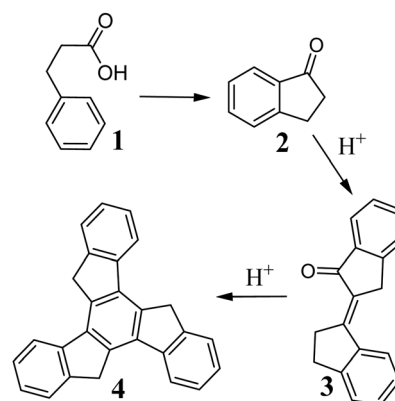
## 2. $C_{3h}$ -Symmetric truxenes

### 2.1. Truxene: synthesis and reactivity

Truxene **4**, for the first time, was accidentally obtained in 1889 by Hausmann during the synthesis of indan-1-one **2** from 3-phenylpropanoic acid **1** (Scheme 1). The mechanism of this reaction, with the participation of the  $\alpha,\beta$ -unsaturated intermediate **3**, was elucidated many years later.<sup>33</sup> This cyclotrimerization of aldol is still the most frequently used method for the synthesis of truxenes.

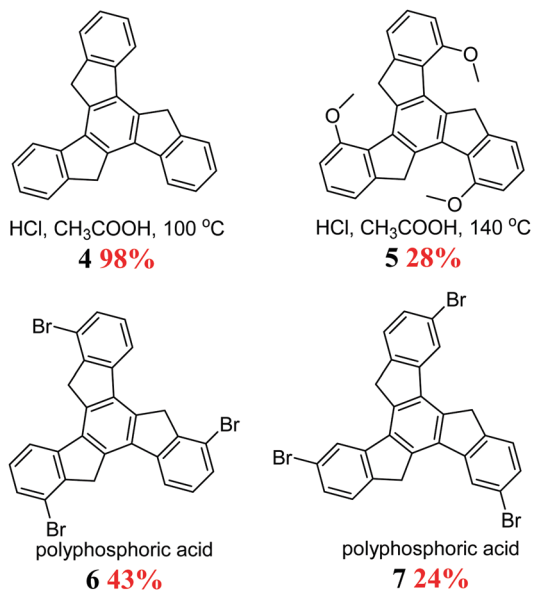
$H^+$  is necessary to initiate condensation, and hence **4** is formed in strong acidic media, e.g., polyphosphoric acid<sup>34</sup> or mixture of conc. AcOH and aqueous HCl.<sup>35</sup> The reaction yield of the latter is a record-breaking 98%. Truxenes are also obtained from appropriately functionalized indan-1-ones to synthesize, for example, hexamethoxy derivatives.<sup>36</sup> Other truxene derivatives were obtained under harsher conditions but with a lower yield (Scheme 2).<sup>37</sup> This can be explained by the negligible solubility of the corresponding  $\alpha,\beta$ -unsaturated ketone.

The described methods require a large excess of acid relative to ketone, but this is not necessary for efficient cyclotrimerization. The use of 3.5 equiv. of p-TsOH and propionic acid in 1,2-dichlorobenzene at 105 °C allows the efficient condensation (59–89%) of indan-1-ones to the corresponding truxenes.<sup>38</sup> Further, using 1 equiv. of  $\text{MeSO}_3\text{H}$  with  $\text{Si}(\text{OEt})_4$  in DCM at room temperature allows the cyclotrimerization of **2** with 80% yield.<sup>39</sup> Indan-1-ones also undergo condensation in the presence of a catalytic amount of Rh(III) complex at 150–200 °C without solvent.<sup>40</sup> The cyclotrimerization of more complexed indanones in the presence of  $\text{POCl}_3$  is worth mentioning.<sup>41</sup> Isomeric compounds **2** and **8** undergo cyclotrimerization to **4** in the presence of  $\text{SiCl}_4$  in EtOH (Scheme 3).<sup>42</sup>



Scheme 1 First truxene synthesis.

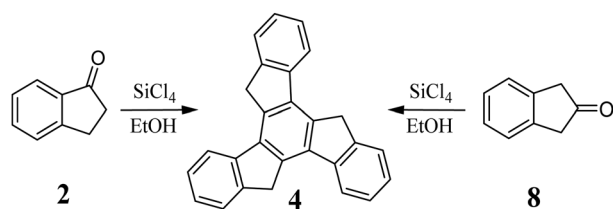




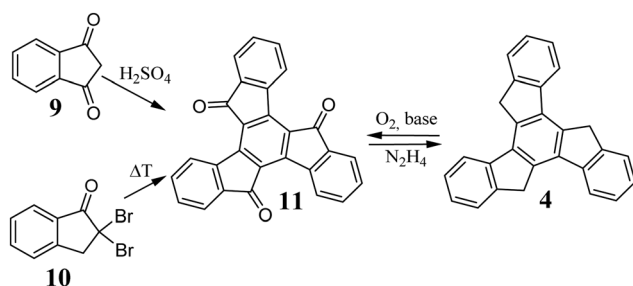
Scheme 2 Indan-1-one cyclotrimerization products, conditions and reaction yields.

However, the broader use of indan-2-ones for the synthesis of truxenes is limited, mainly due to their availability.

The described cyclotrimerization processes allow truxenes that are unfunctionalized in positions 5, 10, and 15 to be obtained. These positions are important for modifying the electronic structure and improving the solubility of truxenes. Indan-1,3-dione **9** in the presence of concentrated H<sub>2</sub>SO<sub>4</sub> forms truxene-5,10,15-trione **11** (Scheme 4).<sup>35</sup> Microwave-assisted cyclotrimerization significantly reduces the reaction time while maintaining a high yield of 77%.<sup>43</sup> Likewise, 2,2-dibromoindan-1-one **10**, under pyrolysis condition, undergoes cyclotrimerization to form **11**.<sup>44</sup> The main advantage of using **9** and **10** is the direct synthesis of



Scheme 3 Cyclotrimerization in the presence of SiCl<sub>4</sub>/EtOH.



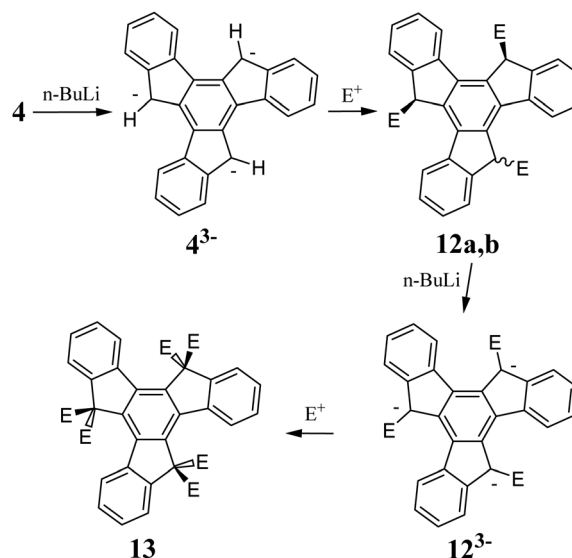
Scheme 4 Synthesis of truxene-5,10,15-trione.

functionalized truxene in positions 5, 10, and 15. The carbonyl groups in **11** undergo ketone-specific reactions, and hence N<sub>2</sub>H<sub>4</sub> can convert it to **4**.<sup>45</sup> Reverse conversion, *i.e.*, oxidation of the methylene moieties of **4** in positions 5, 10, and 15, is also possible. The use of a composite of KOH and graphene<sup>46</sup> or a suspension of KOH in THF<sup>47</sup> in the presence of O<sub>2</sub> efficiently oxidizes **4** to **11**. The base used in this process must be strong enough to ionize the 5, 10, and 15 positions; therefore, KOH can be replaced by Me<sub>4</sub>NOH or K<sub>2</sub>CO<sub>3</sub>.<sup>48</sup> Recent studies indicate that in the presence of light and O<sub>2</sub>, **4** can be oxidized to a monocarbonyl derivative, namely truxene-5-on.<sup>49</sup>

Unsubstituted truxenes display low solubility, which is a direct consequence of their strong  $\pi$ -stacking interactions. Thus, to reduce this intermolecular effect, alkyl substituents are introduced in the 5, 10, and 15 positions. Strong bases can ionize the acidic hydrogen atoms in a five-membered ring. The produced aromatic anions **4**<sup>3-</sup> and **12**<sup>3-</sup> can serve as valuable substrates for further derivatization of the truxene core, for example, C-alkylation (Scheme 5).

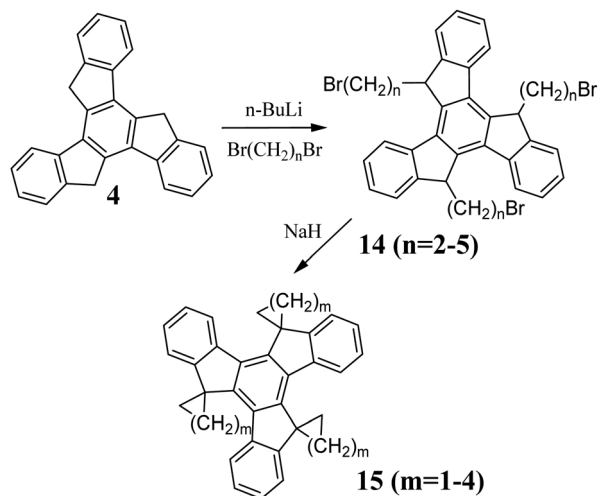
The alkali metal hydrides NaH<sup>50</sup> or KH<sup>51</sup> and organolithium compounds are the most commonly used bases to generate **4**<sup>3-</sup>. In the reaction between **4** and *n*-BuLi, the orange fluorescent **4**<sup>3-</sup> is formed. Subsequent reaction of **4**<sup>3-</sup> with, *e.g.*, alkyl halide, results in a mixture of two diastereomers, containing mainly the anti-product **12a**. The syn-product **12b** can be obtained from **12a** after reacting with *t*-BuOK in *t*-BuOH.<sup>52</sup> In the case that the solubility of the reactants appears to be insufficient, DCM is added to increase their solubility and the isomerization yield. A mixture of **12a** and **b** can be ionized and converted to the corresponding hexa-substituted truxenes **13**. Alkyl or benzyl halides are the most commonly used electrophilic agents. However, by using appropriate dibromoalkanes, spiro systems **15** can be obtained (Scheme 6).<sup>53</sup>

The isolation of products can be troublesome due to their similar polarity after alkylation is performed. Thus, for



Scheme 5 Triple lithiation of **4**.





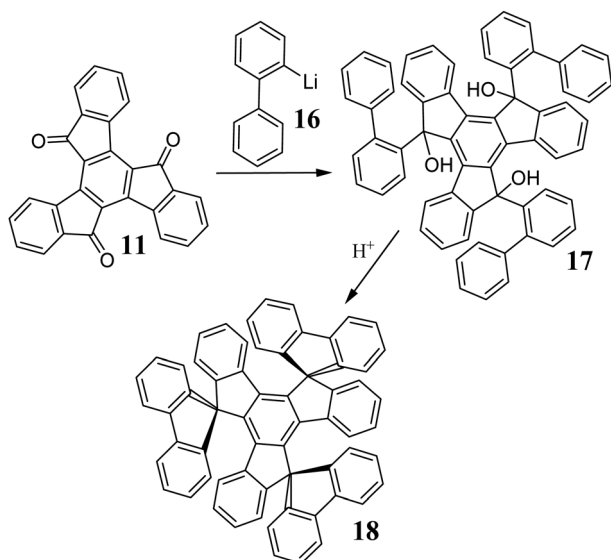
Scheme 6 Synthesis of cycloalkanospirotruxenes.

practical reasons, truxenes are often subjected to exhaustive alkylation to 13 under anaerobic conditions to avoid oxidation.

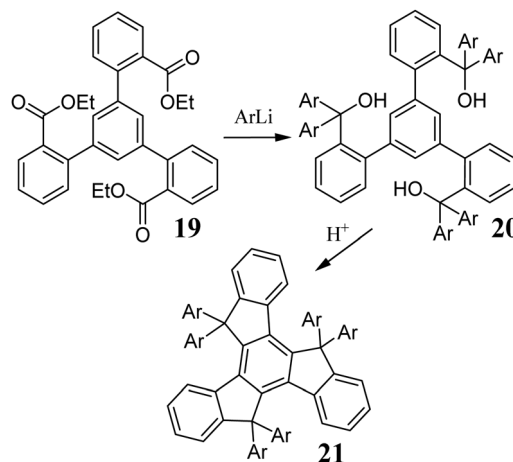
Complementary modifications can be realized *via* the carbonyl groups in 11. As a result of the reaction with both organolithium<sup>54</sup> and organomagnesium<sup>37</sup> compounds, the corresponding trihydroxy derivatives are formed (Scheme 7).

11 undergoes condensation with malononitrile,<sup>55</sup> Wittig-Horner olefination,<sup>56</sup> and reacts with organometallic compounds such as  $\text{PhLi}$ , and more complex derivatives of biphenyl 16,<sup>57</sup> anthracene or phenanthrene.<sup>58</sup> The use of 16 allows the synthesis of more exotic systems, *i.e.*, trispirotruxenes 18. It is worth noting that trispirotruxenes possessing an external alkyl ring can be obtained *via* ring-closing metathesis.<sup>59</sup>

The main limitation of the described methods is the low solubility of 11. Therefore, some modifications may prove challenging to implement. An alternative approach to introduce aryl



Scheme 7 Synthesis of fluorenespirotruxenes.



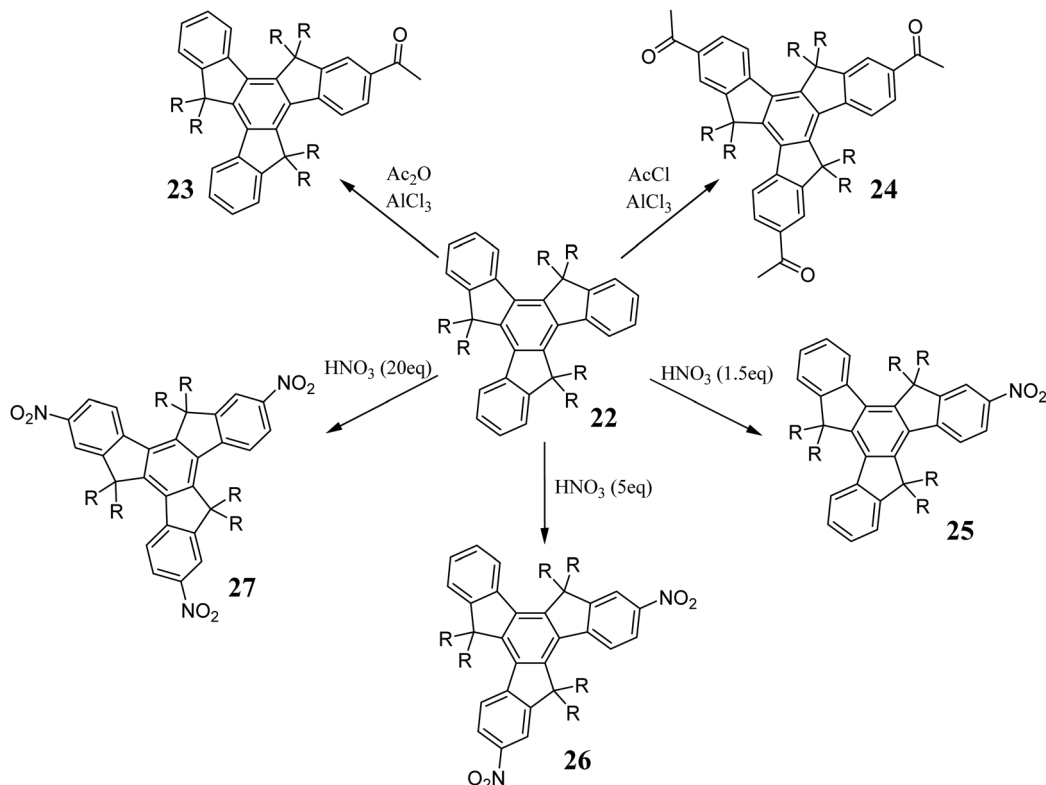
Scheme 8 Synthesis of hexaaryltruxenes.

substituents in the truxene five-membered rings is the addition of an organometallic compound to ester 19 (Scheme 8). The obtained alcohol 20, in the presence of an acid, undergoes cyclization to hexaaryltruxene 21.<sup>60</sup> 20 may also participate in competitive reactions. Cyclization using  $\text{HCl}_{\text{aq}}$  may result in the formation of chlorinated by-products; thus,  $\text{H}_2\text{SO}_4$  or  $\text{MeSO}_3\text{H}$  is suitable. In contrast to 11, compounds 19 and 20 are relatively soluble, making this method attractive for their further functionalization. Truxenes can be functionalized *via* electrophilic substitution at positions 2, 7, and 12 (Scheme 9). In the presence of  $\text{Ac}_2\text{O}$  and  $\text{AlCl}_3$ , 22 undergoes Friedel-Crafts reaction to form 23,<sup>61</sup> which proved to be a valuable substrate in the synthesis of dendrimers.<sup>62</sup> Using excess  $\text{AcCl}$  and  $\text{AlCl}_3$ , 24 is obtained.<sup>63</sup> Truxene also undergoes other electrophilic substitutions, *i.e.*, nitration using  $\text{HNO}_3$  in 1,2-dichloroethane. Mono- 25, di- 26, and trinitro derivatives 27 can be obtained in good yield.<sup>64</sup> Alternatively, the reduction of  $\text{NO}_2$  to  $\text{NH}_2$  allows the further peripheral expansion of the  $\pi$ -electron system.<sup>65,66</sup>

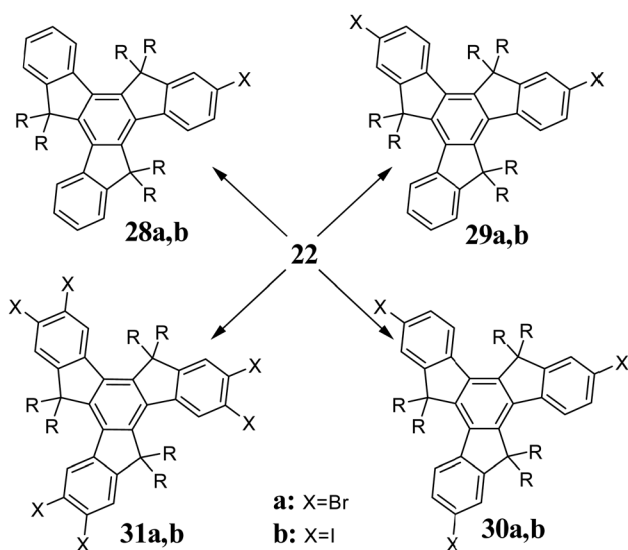
Halogenation is the most common method used for the functionalization of truxenes (Scheme 10). In the presence of *N*-bromosuccinimide (NBS), 22 undergoes monobromination 28a,<sup>67</sup> while using the right stoichiometry of  $\text{Br}_2$ , di- 29a<sup>68</sup> and tribromoderivatives 30a can be obtained.<sup>69</sup> Six-fold bromination occurs in the presence of a catalytic amount of  $\text{I}_2$  31a.<sup>70</sup> Iodination is also possible; however, due to the lower reactivity of  $\text{I}_2$ , the presence of an oxidant is required. Mono-iodination product 28b is obtained using a mixture  $\text{I}_2/\text{H}_5\text{IO}_6$ <sup>71</sup> or  $\text{I}_2/\text{HIO}_3$ .<sup>72</sup> However, excess  $\text{I}_2/\text{HIO}_3$  at 80 °C allows the introduction of two 29b or three 30b iodine atoms. By increasing the iodination temperature to 115 °C, hexaiodotruxene 31b is obtained. 31b is also a product of the reaction between 22 and  $\text{I}_2$  in the presence of PIFA.<sup>73</sup> Obtaining 28 and 29 is achievable by using the appropriate stoichiometry; however, isolating the desired compound can be troublesome. It is interesting that monosubstituted truxenes possessing electron-withdrawing groups such as formyl undergo efficient double halogenation.<sup>74,75</sup>

Halogenated truxenes undergo lithium-halogen exchange, which enables the introduction of a carboxyl<sup>76</sup> or formyl<sup>77,78</sup> group or their conversion to appropriate boronic acids.<sup>79</sup>





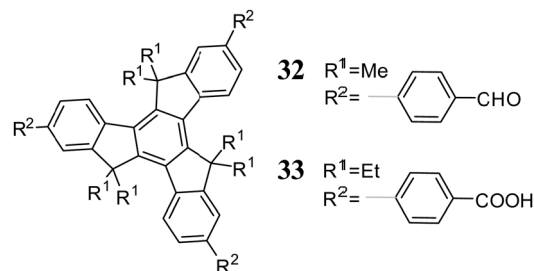
Scheme 9 Electrophilic substitution of truxene.



Scheme 10 Halogenation of truxenes.

Halogen atom replacement with a boronic ester was also carried out catalytically using  $\text{Pd}(\text{dppf})_2\text{Cl}_2$ .<sup>80</sup> Truxenes also undergo direct triple borylation in the presence of  $[\text{Ir}(\text{OCH}_3)(\text{COD})_2]$ .<sup>81</sup> Under Ulman<sup>82</sup> or Buchwald-Hartwig<sup>83</sup> reaction, halogenotruxenes are converted into the corresponding 3° amines. However, the most crucial halogenotruxene transformation is Pd-catalysed coupling. The peripheral functionalization *via* Suzuki reaction allows easy

$\pi$ -electron expansion of the truxene core.<sup>84</sup> Halogenotruxenes react with simple boronic acids<sup>85–88</sup> and  $\pi$ -expanded derivatives.<sup>89–96</sup> The connection of benzoic acid and benzaldehyde is also possible *via* this process.<sup>97</sup> The mentioned Suzuki transformation allows the synthesis of yellow<sup>98</sup> and white<sup>99</sup> polymeric emitters, as well as the creation of ordered porous materials, namely, two-dimensional COFs (covalent organic frameworks) **32**<sup>100</sup> and three-dimensional MOFs (metal-organic frameworks) **33**<sup>101</sup> (Scheme 11). The microwave-assisted coupling of halogenotruxenes with boronic acids allows the introduction of up to six oligofluorene moieties with high reaction yield.<sup>102</sup> The Suzuki reaction allows the direct connection of truxene subunits, leading to truxene-only dendrimers<sup>103</sup> and polymers.<sup>104</sup> An alternative coupling often used to expand the  $\pi$ -electron truxene system is the Sonogashira reaction.<sup>105–110</sup> Other Pd-catalysed couplings, such as the Heck<sup>67</sup> and Negishi<sup>111</sup>

Scheme 11 Structural subunits **32** – COF and **33** – MOF.

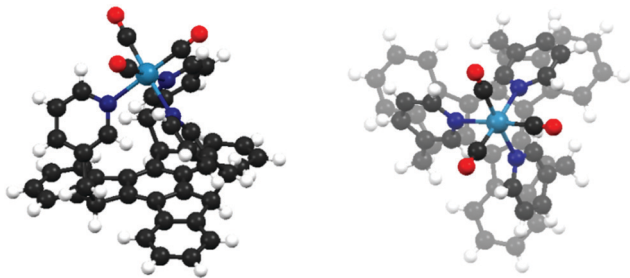


Fig. 2 Structure of carbonyl Re(I) complex.

reactions, are occasionally used for the functionalization of truxenes.

Truxenes decorated with chelating subunits were used to synthesize multi-core Os<sup>2+</sup>, Ru<sup>2+</sup>, and Pt<sup>2+</sup> complexes.<sup>17,112–116</sup> Some of these systems exhibit non-linear optical (NLO) properties. An interesting example of a truxene-based ligand is the 5,10,15-tri(pyrid-3-ylmethyl) derivative, which coordinates the Re<sup>+</sup>, placing it on the C<sub>3</sub> axis (Fig. 2).<sup>117</sup>

The  $\pi$ -expansion of truxenes can lead to uncommon strained systems such as monkey saddle<sup>27</sup> or fullerene fragments, and precursors of C<sub>60</sub><sup>28,118–120</sup> and C<sub>84</sub><sup>120,121</sup> (Fig. 3). Several research groups successfully synthesized spherical molecules. Appropriately functionalized truxenes have been proposed as precursors for the synthesis of short carbon nanotubes.<sup>122</sup>

## 2.2. Truxenes: physicochemical properties and applications

The C<sub>3h</sub> symmetry of the truxene molecule has an immense impact on its photophysical properties. The HOMO and LUMO levels of truxene are double degenerate. This means that the first two electronic transitions, *i.e.*, S<sub>0</sub> → S<sub>1</sub> and S<sub>0</sub> → S<sub>2</sub>, are symmetry forbidden. The fluorescence quantum yield of simple C<sub>3</sub>-symmetric truxenes is relatively low at about 9%. Truxenes also possess a very unusual phosphorescence spectrum with one dominant narrow peak, the origin of which was explained

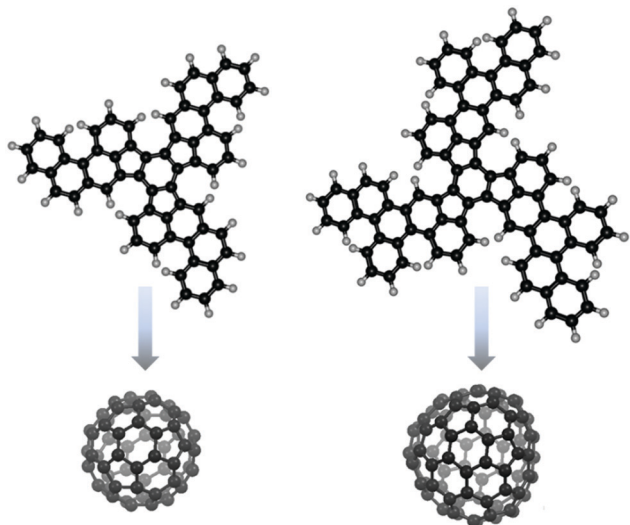
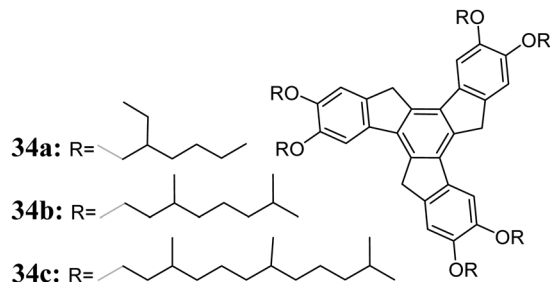


Fig. 3 Truxene-based fullerenes precursors: left – C<sub>60</sub> and right – C<sub>84</sub>.



Scheme 12 NLO liquid crystalline truxenes.

by Baunsgaard *et al.*<sup>123</sup> The T<sub>1</sub> → S<sub>0</sub> transition is forbidden due to multiplicity and symmetry, resulting in a very long phosphorescence lifetime of about 16 s.<sup>124</sup> The truxene moiety exhibits a reversible oxidation process and irreversible reduction.<sup>125</sup> In contrast, in its derivatives, both redox processes are reversible,<sup>47,55,126</sup> which is beneficial for optoelectronics.

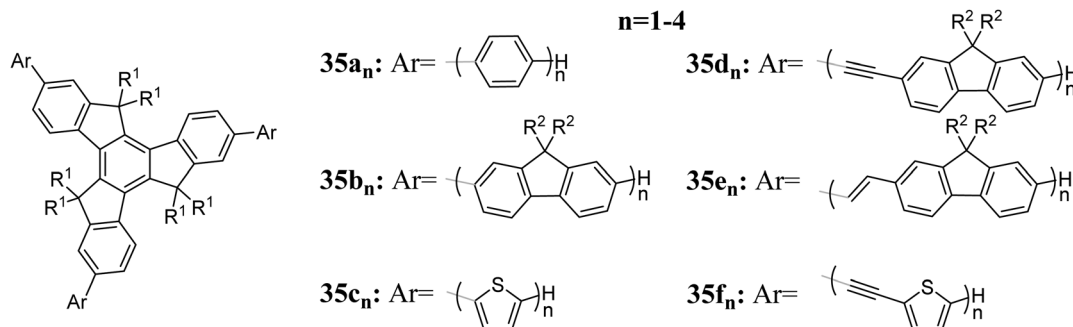
Truxenes having long alkyl chains were the first derivatives thoroughly investigated. They exhibit liquid crystalline properties and rich polymorphism.<sup>127–132</sup> Due to their strong  $\pi$ -stacking interactions, truxenes exhibit a tendency to undergo columnar ordering in the solid state. The aggregation combined with the reversible reduction process of truxene-5,10,15-trione makes it promising for the synthesis of new n-type semiconductors.<sup>133</sup> Recent studies also suggest the possibility of using truxenes decorated with long alkoxy chains in NLO (Scheme 12).<sup>134</sup>

Truxene **35** has been the subject of many application studies (Scheme 13).<sup>135–139</sup> Regardless of the substituent type, **35** has very high fluorescence quantum yields up to 99%.<sup>140</sup> The  $\pi$ -electron system expansion upon oligoaryl chain elongation is visible by the redshift in its absorption and emission spectra.<sup>141,142</sup> **35** is thermally and electrochemically stable,<sup>143</sup> even exhibiting chemiluminescence.<sup>144</sup> These properties make **35** and its derivatives valuable compounds for LEDs,<sup>145</sup> OPVs,<sup>146</sup> and OFETs.<sup>11</sup> They also act as good emitters<sup>147</sup> and light-harvesting dyes.<sup>148,149</sup>

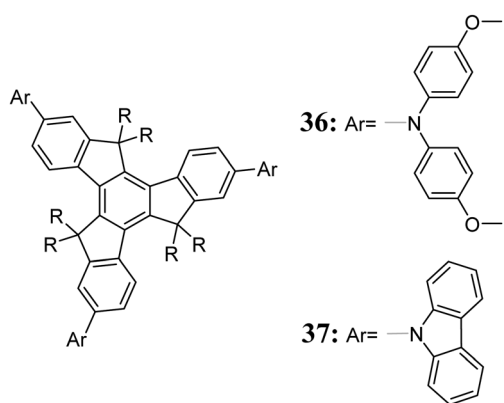
**35b** has also been tested for amplified spontaneous emission (ASE).<sup>150,151</sup> Similar truxene structures substituted by oligofluorenes<sup>152</sup> and oligofluorenes terminated with pyrenes<sup>153</sup> or diphenylamines<sup>154,155</sup> were tested in a blue laser. The non-linear properties of truxenes **35b** and **e** reveal significant two-photon absorption (TPA).<sup>156,157</sup> Theoretical studies suggest that **35c** should also exhibit similar properties.<sup>158</sup> Besides optoelectronic applications, truxenes,<sup>159</sup> truxenes modified by thienyl chains,<sup>160,161</sup> and dendrimeric structures made of them,<sup>162</sup> have been used as stationary phases in gas chromatography.

The presence of aromatic subunits enables tuning of the physicochemical properties of the  $\pi$ -electron system.<sup>163</sup> The introduction of donating subunits increases the electron density significantly in the truxene core, increasing its hole conductivity (Scheme 14).<sup>164–171</sup> Its conducting properties can also be tuned differently. The presence of peripheral long alkoxy chains increases the intermolecular interactions, changing the conductivity of substituted truxenes, resulting in hole<sup>172</sup> or ambipolar<sup>173</sup> conductivity. Donor subunits result in a red shift in the absorption and fluorescence spectra of truxene derivatives.<sup>174</sup> Consequently,





Scheme 13 Oligoaryl truxenes.

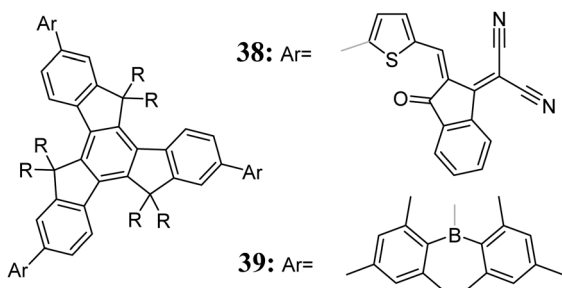


Scheme 14 Examples of electron-rich truxenes.

they can be used as blue emitters in OLEDs<sup>6</sup> and lasers.<sup>175</sup> Recent research indicates that the presence of the truxene core significantly impacts the light-harvesting properties of materials.<sup>15</sup>

Alternatively, an acceptor unit, such as fullerene,<sup>176</sup> attached to truxene, increases its electron conductivity. Current photovoltaic electron-deficient systems do not contain fullerene molecules.<sup>126,133,177–182</sup> However, better electron conductivity is not the only advantage of electron-withdrawing substituents.  $\pi$ -Electron systems equipped with diarylboron substituents **39** (Scheme 15) are characterized by more than 4-fold higher fluorescence quantum yield compared to that with **4**.<sup>183</sup>

The donor properties of dithiole-modified truxene and its characteristic concave shape can be used in noncovalent interaction with fullerene C<sub>60</sub>, which is known for its accepting



Scheme 15 Examples of electron-deficient truxenes.

behavior. This noncovalent donor–acceptor pair is presented in Fig. 4.

Despite the already discussed donor or acceptor substituents for truxene, it is worth paying more attention to covalent D–A systems.<sup>184–188</sup> The common feature of these systems is solvatochromism, resulting from excited-state charge separation.<sup>189</sup> The presence of D–A subunits in OPVs inhibits charge recombination.<sup>190</sup> This feature makes D–A truxenes applicable in dye-sensitized solar cells (DSSC).<sup>191,192</sup>

Due to the high affinity of F<sup>−</sup> to the boron atom, some truxenes can act as fluorescent switches.<sup>193</sup> As the concentration of F<sup>−</sup> increases, the CT state fluorescence intensity decreases in favour of local emission, changing the colour of the emitted light. Besides, some truxenes can detect cations,<sup>194,195</sup> nitro compounds,<sup>196,197</sup> and even proteins containing metalloporphyrin subunits.<sup>198</sup> Recent studies showed that their sensing property is directly related to the presence of the truxene core and the substitution position.<sup>199</sup>

Truxene-based MOFs and COFs can be used for the storage of gases or small molecules,<sup>22</sup> as well as for HCl sensing.<sup>20</sup> Surprisingly, an adequately designed structure may lead to electron conductive materials<sup>200</sup> or water desalination membranes.<sup>201</sup> Some truxene-based polymers show interesting sorption properties, *e.g.*, for CH<sub>4</sub>.<sup>202</sup> Another truxene-based polymeric material exhibited photocatalytic properties<sup>203</sup> and could be applied as solar fuels<sup>204,205</sup> or for the homocoupling of amines.<sup>206</sup>

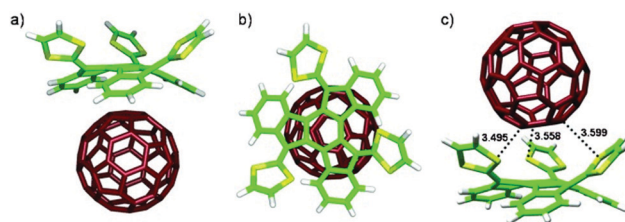


Fig. 4 Structures of the 3 a-C<sub>60</sub> complex calculated at the MPWB1K/6-31G\*\* level. (a) Side view of the preferred configuration. (b) Top view of the same configuration, showing the stack between the central benzene ring of the truxene core and one of the hexagonal rings of C<sub>60</sub>. (c) Side view of the other possible configuration, with C<sub>60</sub> approaching 3 a on the dithiole side. S–C short contacts [Å] are also shown. The carbon atoms of the fullerene are depicted in red for clarity. Reproduced from E. M. Pérez, M. Sierra, L. Sánchez, R. Torres, R. Viruela, P. M. Viruela, E. Orti, N. Martín, *Angew. Chem., Int. Ed.*, 2007, **46**, 1847–1851, with permission from John Wiley and Sons.





An interesting work on the properties of various truxene-based COFs and MOFs was presented by Berta Gómez-Lor and colleagues, as shown in Fig. 5.<sup>207</sup>

Every truxene monomer can be applied to create 2D or 3D materials in multiple ways, where DFT calculations can enable the preselection of suitable monomers. It is worth mentioning that truxene derivatives can be used for the amplification of chirality in discrete molecular assemblies, where one chiral molecule can control the chirality of the entire assembly.<sup>78</sup>

### 2.3. 5,10,15-Trisilatruxene

The preparation of heavier analogues of truxenes has been unattainable for years. However, the silole ring formation development, including the sila-Friedel-Crafts reaction<sup>208</sup> and catalytic silylation,<sup>209</sup> enabled real attempts for the synthesis of 5,10,15-trisilatruxene. In 2017, Ogaki *et al.* synthesized an alkyl derivative of 5,10,15-trisilatruxene **41** (Scheme 16).<sup>124</sup>

The three silicon atoms present in the truxene core do not change the symmetry of the system, and hence the first two-electron transitions, as in truxene, are forbidden. The energy of the HOMO is slightly lower, while that of the LUMO is significantly lower compared to truxene. This is due to the  $\sigma^*-\pi^*$  interaction in the silole ring. Consequently, a redshift in the absorption and emission spectra is observed.

Generally, the presence of silicon atoms does not affect the fluorescence quantum yield but visibly changes the phosphorescent properties. Two intense peaks are present in the spectrum and the phosphorescence lifetime is four-times shorter, *i.e.*,  $\tau_{\text{phos}} \approx 4$  s, than in truxene. Due to the relatively high energy of its  $T_1$  state, **41** can be used as a sensitizer for blue phosphorescent OLEDs. In comparison to their carbon analogues, siloles have



Scheme 16 Synthesis of 5,10,15-trisilatruxene.

better electron conductivity,<sup>210</sup> and hence 5,10,15-trisilatruxenes can be considered semiconductors.

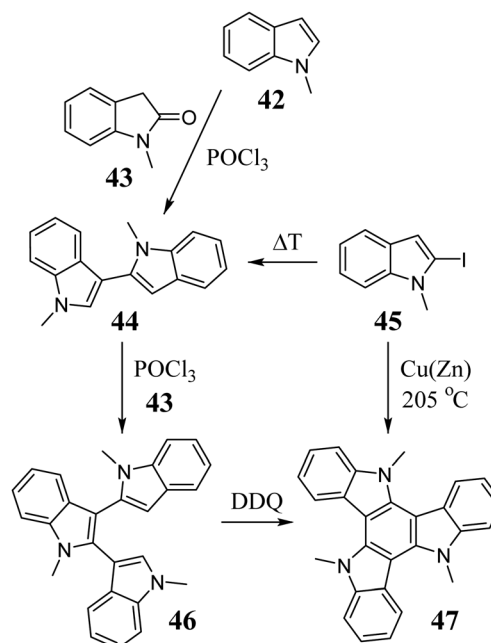
### 2.4. 5,10,15-Triazatruxene: synthesis and reactivity

The 5,10,15-triazatruxene **47** was presented for the first time by Bergman *et al.* concerning the condensation of indole **42** and 2-oxindole **43** (Scheme 17).<sup>211</sup> **47** is a product of a multistep synthesis. It begins from bisindole **44**, which is obtained during thermolysis of 2-iodoindole **45** or *via* the Vilsmeier reaction between **42** and **43**. Another Vilsmeier reaction between **43** and **44** gives trimer **46**, followed by conversion to **47** by cationic radical cyclization, with a total yield of 30.6%. Using activated Cu bronze at 205 °C allowed the conversion of **45** to **47** with 81% yield.<sup>212</sup>

The electron-rich indoles **48a-e**, when treated with  $(\text{NH}_4)_2\text{S}_2\text{O}_8$ <sup>213</sup> or  $\text{Na}_2\text{S}_2\text{O}_8$ ,<sup>214</sup> undergo oxidative cyclotrimerization, leading to isomeric aromatic compounds, *i.e.*, triazatruxene (**49a-e**) and triazaisotruxene (**50a-e**) (Scheme 18). Trimerization in the presence of  $\text{S}_2\text{O}_8^{2-}$  is strongly dependent on the solution pH; hence, the best reaction yields ( $\sim 30\%$ ) are obtained at pH = 1.4. It should also be mentioned that **48f** and **g** under the same reaction conditions lead to triazaisotruxene **50f** and **g** as the



Fig. 5 General chemical structures of the conjugated cores (a) and 2D polymers (b) examined in this study with the notation used throughout the text. Note that the  $T_2$  and  $T_3$  polymers refer to tri-substituted materials with different linkage positions (2, 7, and 12 in  $T_2$  and 3, 8, and 13 in  $T_3$ ), while  $T_{2,3}$  corresponds to hexa-substituted materials in the 2, 3, 7, 8, 12 and 13 positions. Reproduced from S. Gámez-Valenzuela, M. Echeverri, B. Gómez-Lor, J. I. Martínez, M. C. Ruiz Delgado, *J. Mater. Chem. C*, 2020, **8**, 15416–15425, with permission from The Royal Society of Chemistry.



Scheme 17 Synthetic approaches to **47**.



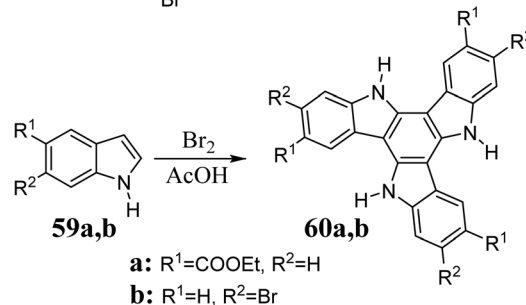
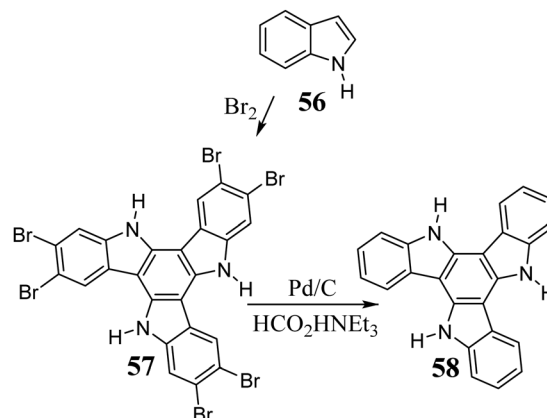
Scheme 18 Oxidative cyclotrimerization of **48**.

only cyclotrimer, respectively. However, due to the large share of byproduct **50** (yield ~20%), oxidative cyclotrimerization may not be an attractive method for the synthesis of 5,10,15-triazatruxenes.

In 2009, Ginnari-Satriani *et al.* reported the one-step synthesis of 5,10,15-triazatruxene **52** from 2-oxindole **51** (Scheme 19).<sup>215</sup> The result of this reaction is highly dependent on both the temperature and the concentration of POCl<sub>3</sub>. As the concentration of POCl<sub>3</sub> increases, the yield of cyclotrimer **52** decreases in favour of cyclotetramer formation **53**.<sup>216</sup> The discovery of this method initiated further development, which allows the condensation of substituted 2-oxindoles **54**.<sup>16,217,218</sup>

Indole **56** in the presence of Br<sub>2</sub> undergoes cyclotrimerization to 5,10,15-triazatruxene. The triazatruxene core is highly reactive towards electrophilic substitution and with excess Br<sub>2</sub>, leads to the hexabromo derivative **57**.<sup>219</sup> After the debromination of **57** in the presence of Pd/C and HCOOHNEt<sub>3</sub>, **58** can be obtained (Scheme 20).<sup>220</sup> Alternatively, some deactivated indoles can be synthesized *via* cyclotrimerization in AcOH in the presence of Br<sub>2</sub>.<sup>221</sup>

As a result of the reaction between indole and NBS, polybrominated 5,10,15-triazatruxenes are obtained. After debromination,



Scheme 20 Bromine-promoted indole cyclotrimerization.

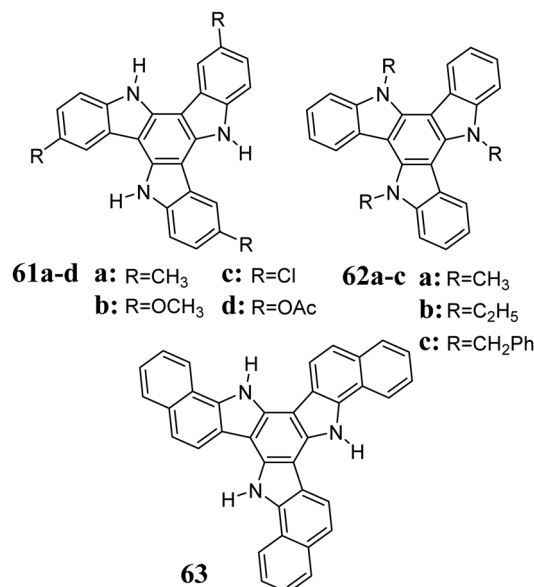
they lead to functionalized derivatives **61**, **62** and **63** (Scheme 21).<sup>222</sup>

5,10,15-Triazatruxene is very reactive toward electrophilic substitution. The most reactive positions are located opposite the nitrogen atom (3, 8, and 13 – green dots, Fig. 6). Alternatively, in the presence of excess electrophile, the substitution may proceed further at positions 2, 7 and 12 (blue dots).

5,10,15-Triazatruxene, in the presence of TfOH, reacts with 3° aromatic alcohols *via* triple electrophilic substitution.<sup>223</sup>



Scheme 19 2-Oxindole condensation.



Scheme 21 Indole condensation products.





Fig. 6 Positions susceptible to electrophilic attack in 5,10,15-triazatruxene.

Upon treatment with  $\text{SnCl}_4/\text{CHCl}_2\text{OCH}_3$ , 5,10,15-triazatruxene undergoes formylation, leading to trialdehyde **65**.<sup>18</sup> The formyl group was used for further functionalization, enabling the synthesis of D-A system **66** and BODIPY and 5,10,15-triazatruxene hybrids **67** (Scheme 22).<sup>224</sup>

Bromination is the primary electrophilic substitution reaction to which 5,10,15-triazatruxene is subjected. Three factors including appropriate stoichiometry, NBS as the brominating agent, and a lower temperature are relevant to obtain greater control over the final composition of the reaction mixture. Accordingly, the appropriate mono- **68**,<sup>217</sup> di- **69**,<sup>225</sup> or tribromo derivative **70**<sup>226</sup> can be obtained. **68** is also a product of the partial debromination of **70** in the presence of  $\text{HCOONa}$  and Pd (Scheme 23).

As a result of the coupling between bromotriazatruxenes **71** and boronic acids,  $\pi$ -electron-expanded, efficient blue emitters were obtained (Scheme 24).<sup>227–231</sup> The Suzuki reaction can be performed in the presence of microwave radiation.<sup>226</sup> **71** also undergo catalytic halogen to boron exchange.<sup>232</sup>

Suzuki coupling allows the synthesis of robust 5,10,15-triazatruxenes.<sup>233</sup> However, desirable products for optoelectronics



Scheme 23 Bromination of 5,10,15-triazatruxene.

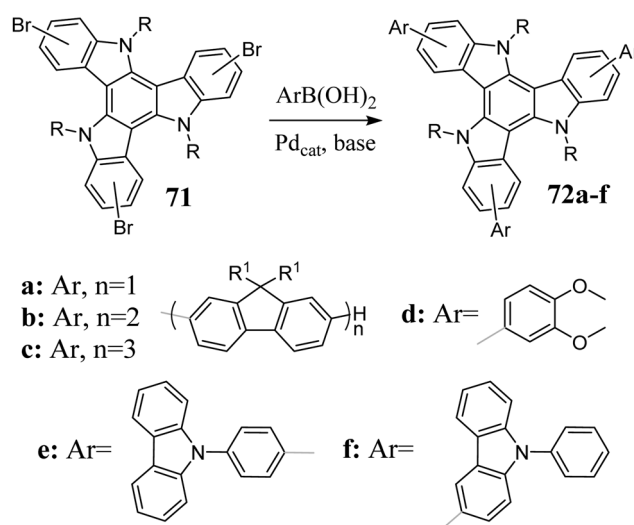
can be obtained *via* alternative methods such as the Sonogashira reaction<sup>234,235</sup> and microwave-assisted Stille coupling (Scheme 25).<sup>236</sup> It should be mentioned that 5,10,15-triazatruxenes unprotected at the nitrogen atom undergo the Buchwald-Hartwig reaction.<sup>237,238</sup>

A significant reaction that **58** undergoes is *N*-alkylation under basic conditions. This crucial transformation in 5,10,15-triazatruxene chemistry allows protection of reactive positions and increases the product solubility. Strong bases such as  $\text{KOH}$ ,<sup>239</sup>  $\text{NaH}$ ,<sup>234</sup> *t*-BuOK,<sup>13</sup> and *n*-BuLi<sup>235</sup> are used as ionizing agents (Scheme 26). Anion **75**, formed during ionization, is extremely easily oxidized, accompanied by a change in solution color to sapphire. Therefore, its deprotonation is performed under strict anaerobic conditions.

Various types of chlorides, bromides, and iodides can serve as alkylating reagents.<sup>240</sup> Benzyl moieties are attractive for protecting nitrogen atoms because they can be easily removed afterward.<sup>234</sup> It is also worth mentioning that the use of an

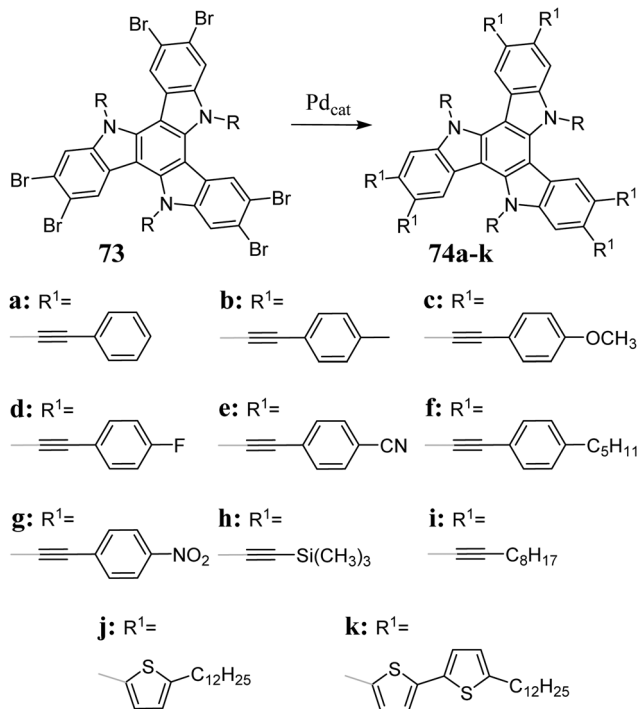


Scheme 22 Synthesis of 5,10,15-triazatruxene **65** and its reactivity.

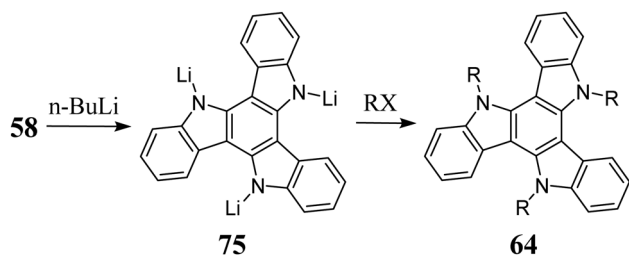


Scheme 24 5,10,15-Triazatruxenes obtained by the Suzuki reaction.





Scheme 25 Sonogashira and Stille coupling products.



Scheme 26 N-Alkylation of 5,10,15-triazatruxene.

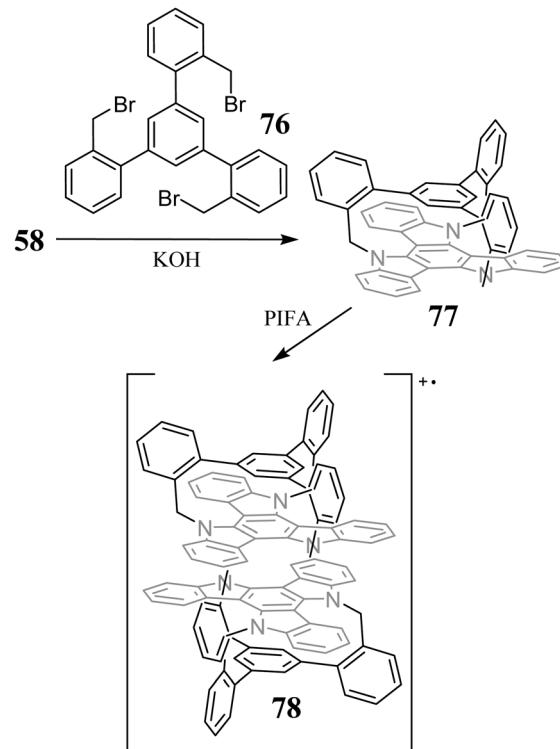
appropriate alkylating agent increases the product solubility in organic solvents and water.<sup>241</sup>

An exciting example of **58** N-alkylation is its reaction with benzyl bromide **76**, resulting in cyclophane **77**. Further reaction with PIFA leads to the stable cation radical **78**, located at two  $\pi$ -stacking triazatruxene subunits (Scheme 27).

N-Alkylation was used to expand the aromatic system. Compounds **79**, due to Pd-catalyzed intramolecular arylation, are transformed into  $\pi$ -expanded systems **80** (Scheme 28).<sup>220</sup> It is worth mentioning that **80** adsorbed on the surface of Pt at 750 °C undergoes cyclodehydrogenation, leading to the formation of the spherical molecule C<sub>57</sub>N<sub>3</sub>, triazafullerene.<sup>242</sup>

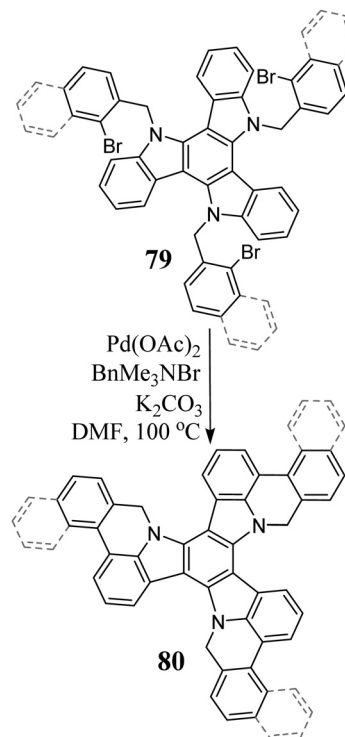
## 2.5. 5,10,15-Triazatruxene: physicochemical properties and applications

In 5,10,15-triazatruxene, the same as in truxene, the first two-electron transitions are symmetry forbidden, reflecting a low fluorescence quantum yield (QY = 3%).<sup>243</sup> A reduction in its HOMO–LUMO gap causes a clear redshift in its absorption and



Scheme 27 Synthesis of cyclophane and stable cation radical.

emission spectra compared to truxene. The relatively high energy of its HOMO level is responsible its reversible oxidation, which combined a with its significant tendency to aggregate,

Scheme 28 Synthesis of  $\pi$ -expanded 5,10,15-triazatruxenes.

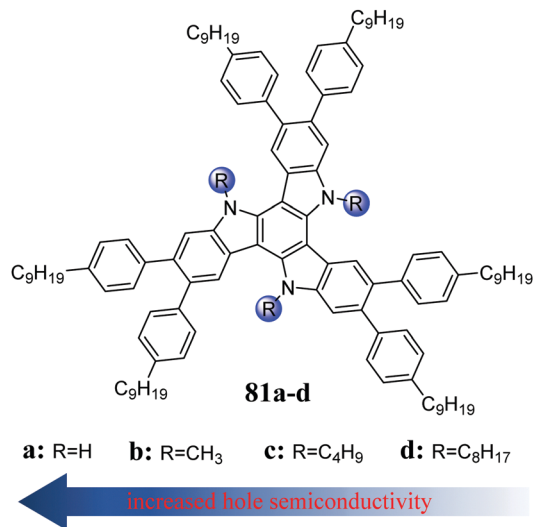


Fig. 7 Increase in conductivity of 5,10,15-triazatruxenes.

leads to high hole conductivity, characteristic for this type of system. Alternatively, the phosphorescence spectrum indicates that the  $T_1$  state of **58** is much more populated, in contrast to **4**. An efficient  $S_1 \rightarrow T_1$  intersystem transition is responsible for the low fluorescence quantum yield.

*N*-Alkylation of **58** slightly affects its optoelectronic properties in the solution but causes evident structural changes in the solid state. The presence of an alkyl chain deforms the 5,10,15-triazatruxene core from planarity,<sup>244</sup> increasing its intermolecular distances and limiting effective  $\pi$ -stacking interactions. However, further elongation of the alkyl chain results in columnar ordering. This behaviour results from the increasing interactions between the alkyl chains and  $\pi$ -system.<sup>10</sup> An exciting example illustrating the aggregation upon alkyl chain elongation is the increase in photocurrent generation observed in a tri(*n*-octyl) derivative.<sup>245</sup> In turn, introducing a branched alkyl chain increases the solubility but significantly limits the  $\pi$ -stacking interactions, decreasing the hole conductivity.<sup>246</sup> However, *N*-alkylation does not always lead to strong  $\pi$ -stacking interactions. If the system is already peripherally functionalized (**81**), the opposite effect is observed, where if the alkyl chain is shortened, the hole conductivity increases (Fig. 7).<sup>247</sup>

The self-assembly of 5,10,15-triazatruxenes<sup>248</sup> was employed to create optical waveguides<sup>249</sup> and design new semiconductor materials for use in prototypical organic thin-film transistors,<sup>250</sup> organic field-effect transistors<sup>12,251,252</sup> and OPVs.<sup>253</sup> In the case of OPVs, **47** or **58** are hole-transporting materials (HTM) and their efficiency increased by 26% compared to the reference devices.<sup>253</sup> The desirable properties of 5,10,15-triazatruxenes result directly from their electronic structure. The relatively low energy of their HOMO level allows effective hole conductivity,<sup>25</sup> while the high energy of their LUMO level limits electron leakage;<sup>254</sup> therefore, they can be used as a cheap HTMs.<sup>255,256</sup> The semi-conductivity of 5,10,15-triazatruxenes can be modulated by increasing their degree of aggregation *via* peripheral functionalization<sup>228,235,257–259</sup> or the presence of donor subunits

(Scheme 29).<sup>260–264</sup> Devices based on functionalized systems can achieve a photocurrent generation efficiency of up to 18.8%.<sup>265</sup>

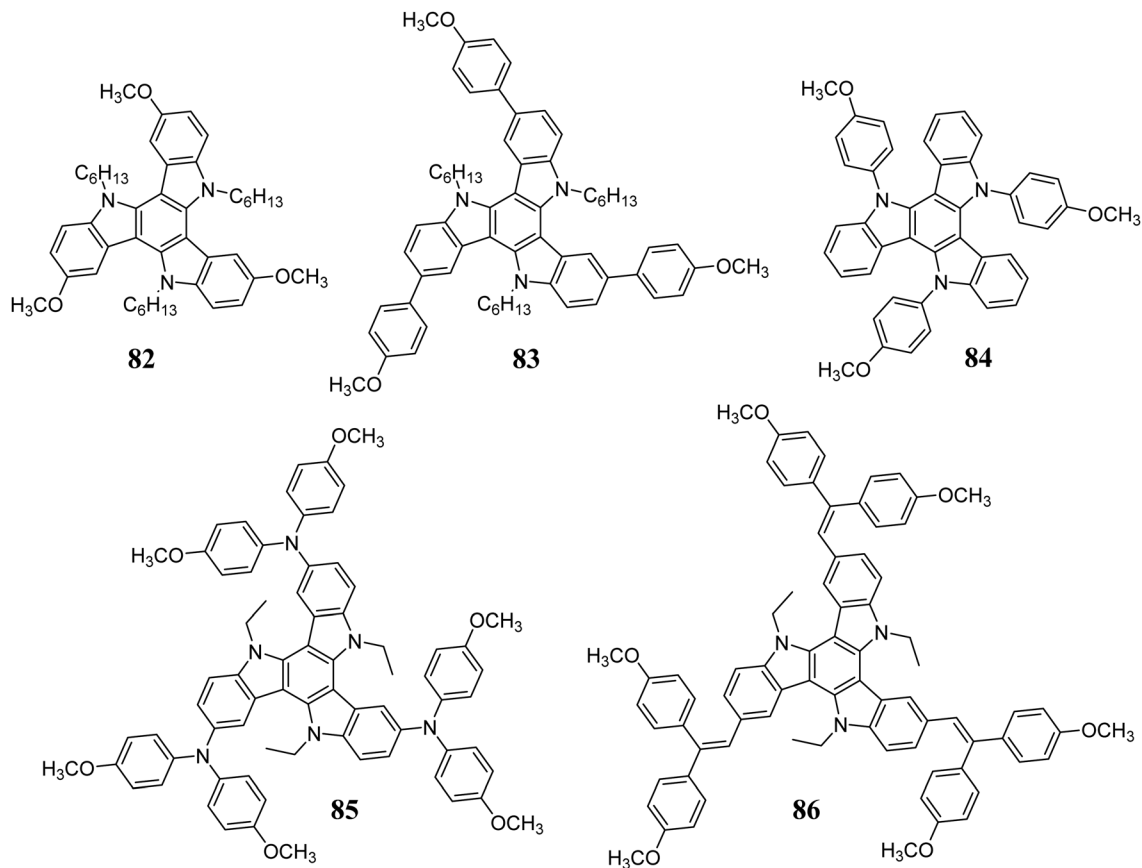
The use of 5,10,15-triazatruxenes in OPVs is not only limited to their semiconductive properties. Some derivatives were used in DSSCs.<sup>14</sup> Due to their aggregation and strong intramolecular interactions, it was possible to obtain a high loading of 5,10,15-triazatruxene-based dye at the  $TiO_2$  surface, improving the performance of the prototype DSSC device.<sup>266</sup> Alternatively, the combination of BODIPY with the 5,10,15-triazatruxene core results in blue dyes with a molar absorption coefficient of  $10^6 \text{ M}^{-1} \text{ cm}^{-1}$ . These systems can serve as light-harvesting materials.<sup>217</sup> The introduction of acceptor subunits<sup>13,267–269</sup> increases the electron conductivity, allowing more balanced charge transport inside the DSSC device.

Functionalization of 5,10,15-triazatruxene with oligothiophene subunits results in materials with good hole conductivity.<sup>270</sup> Alternatively, oligofluorene 5,10,15-triazatruxenes are characterized by a high fluorescence quantum yield<sup>231</sup> and exhibit solvatochromism.<sup>226</sup> The introduction of carbazoles has a similar effect on their spectroscopic properties such as oligofluorene and improves their thermal stability.<sup>271</sup> A redshift, which is associated with oligoaryl chain elongation, was investigated theoretically by Zhang *et al.* (Scheme 30).<sup>272</sup> They performed calculations on systems with 1 to 4 oligoheterofluorene subunits **87**. It was found that regardless of the heteroatom introduced, the HOMO level is mainly located at the 5,10,15-triazatruxene core and its energy practically does not change upon elongation of the substituents. However, extending the oligoaryl chain lowers the LUMO level energy, with a simultaneous shift in the electron density from the triazatruxene core to the oligoaryl chain. The spatial separation of the HOMO and LUMO orbitals explains the solvatochromism observed in the oligofluorene 5,10,15-triazatruxenes.

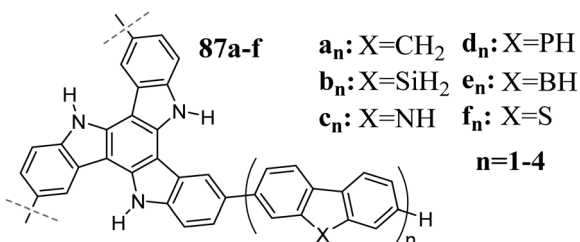
5,10,15-Triazatruxenes are used to create D–A systems, exhibiting thermally activated delayed fluorescence (TADF),<sup>7,273,274</sup> which is utilized in new-generation OLEDs. The presence of triazine subunits in systems **88** and **89** (Scheme 31) results in a redshift in their emission, high photoluminescence quantum yield of about 87%, and an energy difference between  $S_1$  and  $T_1$  equal to 23 meV.<sup>275</sup> Green OLEDs containing **88** or **89** in the emissive layer are characterized by an external quantum efficiency of 31.4%. Moreover, a properly designed D–A system can act as the sensitizer in TADF OLEDs.<sup>276</sup>

The dibenzo[*b,d*]thiophene sulfone-based D–A system **90** exhibits a very short delayed fluorescence decay time.<sup>8</sup> This phenomenon is attributed to about 30 different couplings between the  $S_1$  and  $T_1$  states. Very fast  $T_1 \rightarrow S_1$  conversion results in slight energy loss, and this the photoluminescence quantum efficiency is close to 100%. Penfold *et al.* explained the efficient TADF process in D–A systems based on **90**.<sup>277</sup> D–A systems can be utilized as TADF emitters or NLO materials.<sup>18,19</sup> These compounds show increased TPA, resulting from the spatial separation between the excited and ground states. It was found that the cross-section value for TPA also depends on the position of the acceptor subunit, where **92** exhibits stronger TPA than **93** (Scheme 32).<sup>278</sup> It is worth mentioning that the NLO properties of 5,10,15-triazatruxenes have been successfully used in cell imaging.<sup>279</sup>





Scheme 29 5,10,15-Triazatruxene-based HTMs.



Scheme 30 Tri(oligoheterofluorene) 5,10,15-triazatruxenes.

5,10,15-Triazatruxene was also used to create macromolecular systems such as COFs,<sup>280</sup> MOFs,<sup>281,282</sup> and polymers.<sup>283,284</sup> 5,10,15-Triazatruxene-based polymers can be used as capacitor materials.<sup>284</sup> Some COFs<sup>280</sup> and polymers<sup>285</sup> exhibit higher selectivity towards CO<sub>2</sub> adsorption compared to N<sub>2</sub> or can store H<sub>2</sub> (Fig. 8).<sup>23</sup> The storage capacity of triazatruxene polymers increases in the presence of Li<sup>+</sup> ions. Thus, it is crucial to redistribute Li<sup>+</sup> ions homogeneously in the material, which is achieved by cation-π interactions.

Some of these substances exhibit fluorescence quenching upon interaction with electron-deficient systems.

This property inspired the synthesis of low molecular weight and polymeric materials for the detection of explosives.<sup>286-288</sup> Adequate peripheral functionalization allowed the detection of

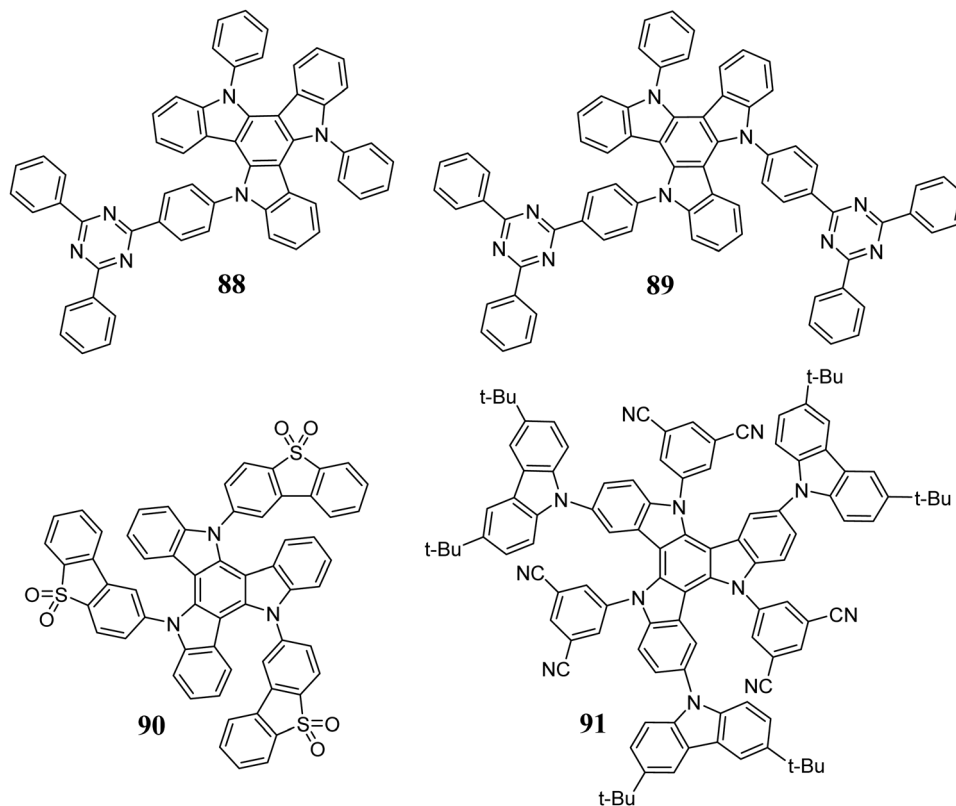
HCl<sup>289</sup> and N<sub>2</sub>H<sub>4</sub> vapors.<sup>290</sup> 5,10,15-Triazatruxene, due to its semiconductive properties, has been used in the synthesis of new, thermally stable polymeric HTMs.<sup>291-293</sup> A 5,10,15-triazatruxene-based microporous polymer could capture heavy metals.<sup>294</sup> A similar interaction with Li<sup>+</sup> cations resulted in a significant increase in the electrical capacity of the polymeric anode.<sup>24</sup> Interactions between 5,10,15-triazatruxene and Fe<sup>2+</sup>/<sup>295</sup> or Zn<sup>2+</sup>/<sup>296</sup> connected with iminopyridyl led to interesting chiral, tetrahedral molecules. Alternatively, the rational design of the molecule may lead to Al<sup>3+</sup>, Cr<sup>3+</sup> and Fe<sup>3+</sup> sensors.<sup>297</sup> 5,10,15-Triazatruxene peripherally decorated with carboxyl groups can be used to modify the surface of TiO<sub>2</sub>, enhancing the electron injection in DSSCs.<sup>298</sup>

5,10,15-Triazatruxene modified by mannose<sup>21</sup> or lactose<sup>299</sup> was used for sensing concanavalin A. 5,10,15-Triazatruxene, upon *N*-alkylation with alkylpiperidine chains, becomes soluble in water and shows amphiphilic properties.<sup>215,300</sup> These substances also have enormous affinity and selectivity toward DNA G-quadruplexes, creating new anti-cancer drugs.<sup>301,302</sup>

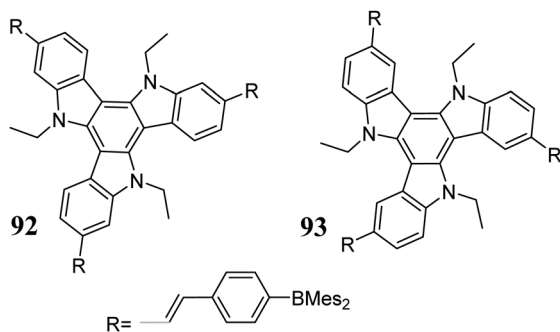
## 2.6. 5,10,15-Triphosphatruxene

5,10,15-Triphosphatruxene has been synthetically unavailable for years. One of the problems arising during the formation of the phosphole ring is that the known methods are not stereo-selective. The phosphorus atom in the phosphole ring, unlike the nitrogen atom in pyrrole, has sp<sup>3</sup> hybridization, becoming a





Scheme 31 Triazatruxene-based D–A systems.



Scheme 32 Isomeric D–A systems exhibiting NLO properties.

potential stereogenic centre. The 5,10,15-triphosphatruxene molecule has three stereogenic phosphorus atoms, but due to its symmetry, the number of possible stereoisomers is reduced to four (Scheme 33).

In 2014, Kojima *et al.*<sup>303</sup> synthesized this complex system *via* aromatic nucleophilic substitution to obtain a mixture of *syn* **94** and *anti* **95** isomers in a ratio of about 1 : 15. However, due to the similar properties of these diastereomers, their separation was complicated. Therefore, their crude mixture was subjected to subsequent oxidation. This procedure enabled crystallization of the pure oxidized isomer *anti* **98** (Scheme 34). Alternatively, upon sublimation of a crude mixture of **94** and **95**, it underwent complete conversion to the thermodynamically more stable isomer **94**. 5,10,15-

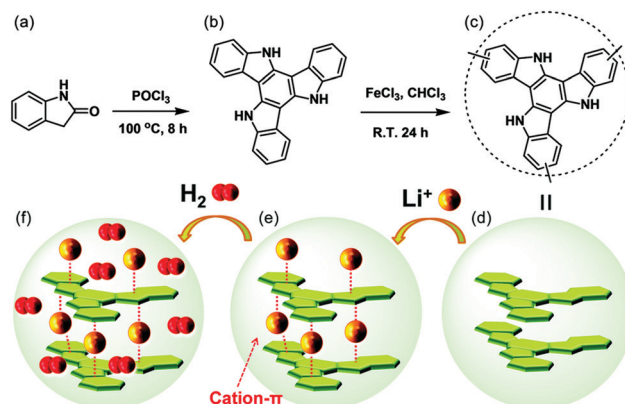


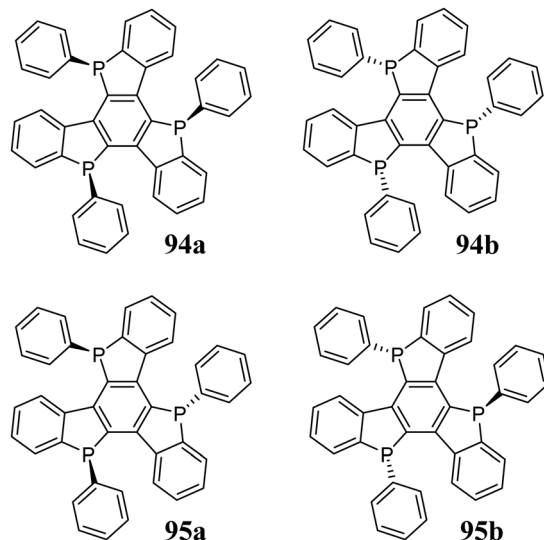
Fig. 8 (a)–(c) Synthetic route for the conjugated microporous polymer PTAT. Schematic representation showing the installation of lithium-doped CMP Li<sup>+</sup>–PTAT through point-to-face cation– $\pi$  interactions (d and e) and its hydrogen adsorption (f). Reproduced from L. Yang, Y. Ma, Y. Xu, G. Chang, *Chem. Commun.*, 2019, **55**, 11227–11230 with permission from The Royal Society of Chemistry.

Triphosphatruxene isomers differ in the symmetry of their molecule. The *syn*-isomer has  $C_3$  symmetry, whereas the *anti*-isomer  $C_1$ . Therefore, different spectroscopic properties are expected.

## 2.7. 5,10,15-Trioxatruxene

The first report on the synthesis of 5,10,15-trioxatruxenes is dated 1984, when Destwde *et al.* obtained several derivatives of





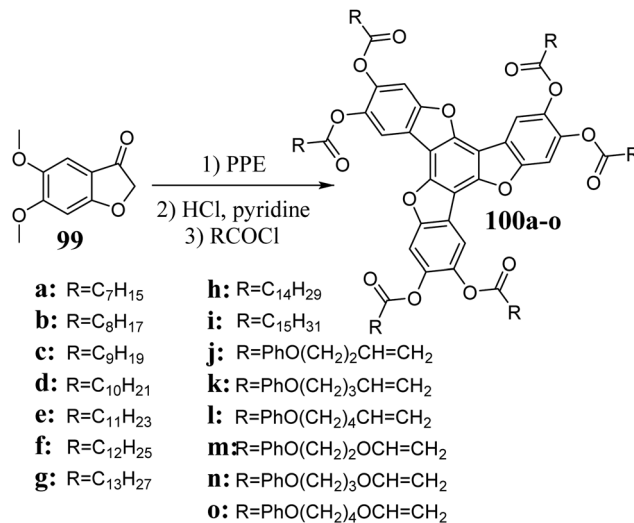
Scheme 33 5,10,15-Triphosphatruxene stereoisomers.

this heterocyclic system.<sup>304</sup> Compounds **100** are products of benzo[*b*]furan-3-one **99** cyclotrimerization in the presence of PPE (Scheme 35). After deprotection of the hydroxyl groups, 5,10,15-trioxatruxene can be further modified to increase its solubility.

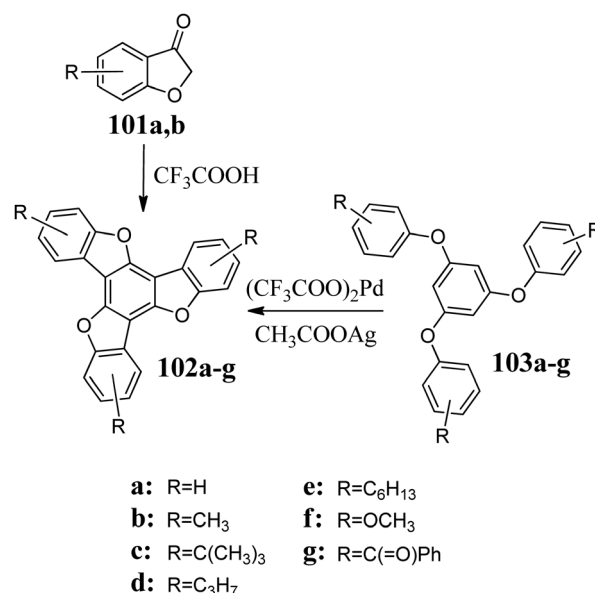
The 5,10,15-trioxatruxenes **102a** and **b** were synthesized using a similar procedure. To carry out the cyclotrimerization of **101a** and **b**,  $\text{CF}_3\text{COOH}$ <sup>305</sup> was used instead of PPE, as mentioned above (Scheme 36).

The described methods were used to synthesize several 5,10,15-trioxatruxene monomers, **100j–o**, containing peripheral polymerizable moieties, making it possible to produce a cross-linked polymer (Scheme 35).<sup>306</sup>

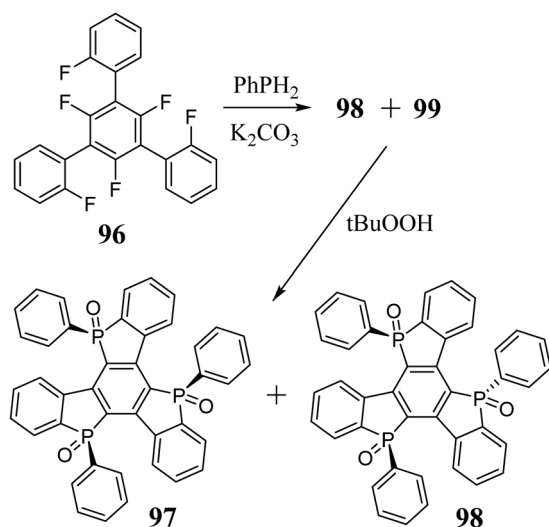
Sato *et al.* refined the synthesis of hexahydroxy-5,10,15-trioxatruxene, enabling the isolation of the condensation products and avoiding chromatography. Thus, this method is



Scheme 35 Synthesis of 5,10,15-trioxatruxene ester derivatives.



Scheme 36 Synthesis of 5,10,15-trioxatruxenes.

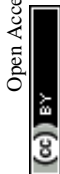


Scheme 34 Synthesis of 5,10,15-triphosphatruxenes.

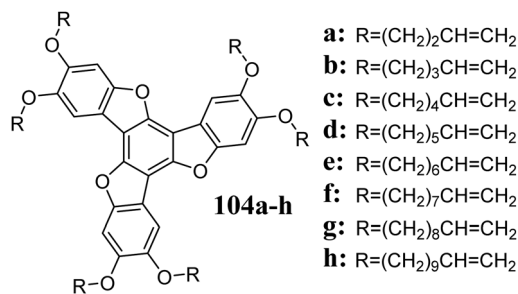
attractive for industrial applications.<sup>307</sup> Sato observed that during deprotection, partial oxidation to quinone occurs. 1,3,5-Triaryloxybenzenes **103a–g**, in the presence of  $(\text{CF}_3\text{COO})_2\text{Pd}/\text{CH}_3\text{COOAg}$ , are converted to **102** in high yield (Scheme 36).<sup>308</sup> However, for derivatives containing donor or acceptor groups, the efficiency of oxidative coupling is relatively low. An exciting example of the efficient synthesis of **102a** is the use of aromatic nucleophilic substitution.<sup>124</sup>

Similar to the previously described systems, the first two electronic transitions in 5,10,15-trioxatruxene are symmetry forbidden.<sup>124</sup>

5,10,15-Trioxatruxene is characterized by a relatively low fluorescence quantum yield of  $\sim 17\%$ . Alternatively, the shape of its phosphorescence spectrum suggests the presence of







Scheme 37 5,10,15-Trioxatruxene-based photopolymerization monomers.

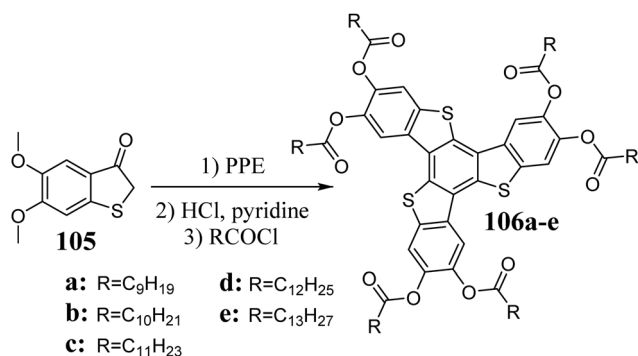
strong coupling between the T<sub>1</sub> and S<sub>0</sub> oscillation states. Moreover, the phosphorescence lifetime of about 5.4 s indicates the forbidden nature of the T<sub>1</sub> → S<sub>0</sub> transition due to the spin multiplicity and the symmetry of the orbitals.<sup>124</sup> **102c** was examined towards electron mobility.<sup>309</sup> The presence of *t*-butyl groups limits the intermolecular interactions, increasing the solubility of the system and making the oxidation process reversible.<sup>308</sup>

Alkylated 5,10,15-trioxatruxenes exhibit liquid-crystal properties and rich polymorphism.<sup>304</sup> The self-assembly of **102a** and its liquid crystalline derivatives toward columnar ordering, combined with reversible oxidation, allows their use as p-type semiconductors. Substituted 5,10,15-trioxatruxenes, containing double bonds on their peripheral alkyl chains, have been used to synthesize cross-linked polymers,<sup>306</sup> while **104** were used as photopolymerization agents, creating so-called “self-healing” LCDs (Scheme 37).<sup>310</sup>

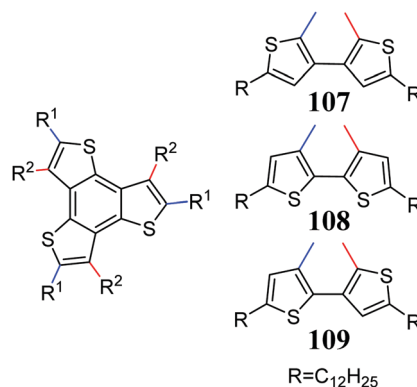
## 2.8. 5,10,15-Trithiatruxene

Peripherally substituted 5,10,15-trithiatruxenes **106** were described for the first time in 1985 by Nguyen *et al.*<sup>311</sup> Their synthesis was based on the acidic condensation of substituted benzo[*b*]thiophen-3-one, **105**, in the presence of PPE (Scheme 38).

Egestad *et al.* showed that the treatment of benzo[*b*]thiophen-3-one with HCl in AcOH leads to a complex mixture of dimeric, trimeric, and tetrameric systems.<sup>312</sup> The same research group performed the cyclotrimerization of 3-acetoxybenzo[*b*]thiophene in CF<sub>3</sub>COOH. They obtained 5,10,15-trithiatruxene in a yield of 13%.<sup>305</sup> 5,10,15-Trithiatruxenes are



Scheme 38 Synthesis of 5,10,15-trithiatruxene ester derivatives.



Scheme 39 5,10,15-Trithiatruxene-based ambipolar semiconductors.

cyclization products of appropriate thioethers in the presence of (CF<sub>3</sub>COO)<sub>2</sub>Pd/CH<sub>3</sub>COOAg at elevated temperatures. Thus, isomeric *t*-butyl peripherally functionalized 5,10,15-trithiatruxenes were obtained. Unfortunately, the reaction yields were much lower than that observed in the case of their oxygen counterparts.<sup>309</sup>

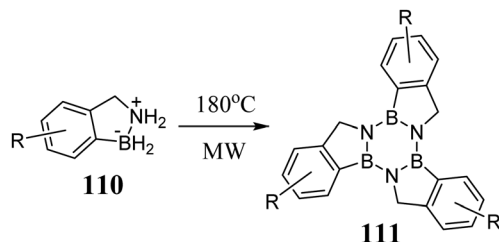
Similar to other symmetrical systems, 5,10,15-trithiatruxene reveals the first two electronic transitions forbidden by symmetry. The presence of sulfur atoms increases the intersystem crossing, resulting in phosphorescence in the solid state at room temperature.<sup>309</sup> Miura *et al.* measured the phosphorescence spectra of two *tert*-butylated trithiatruxenes. The results are eye-catching. The phosphorescence of trithiatruxenes in PMMA films was only observed under vacuum. The authors measured the phosphorescence at low temperatures in methylcyclohexane. They observed almost pure phosphorescence (with minimal fluorescence signal) under these conditions for trithiatruxenes.

Hexa-substituted 5,10,15-trithiatruxenes, like their oxygen analogs, are characterized by rich polymorphism and columnar ordering in the solid state.<sup>311,313</sup> This property has been exploited in epoxy resins, encapsulation, and electronic and structural laminates.<sup>314</sup> Currently, due to the dynamic development of optoelectronics, some 5,10,15-trithiatruxene derivatives can be used in OLEDs,<sup>315,316</sup> OFET,<sup>317</sup> and OPVs.<sup>318</sup> The expanded, liquid-crystalline 5,10,15-trithiatruxene derivatives **107–109** developed by Aida *et al.* tend to self-assemble, increasing their semiconductive properties and leading to balanced, ambipolar conductivity of 0.18 cm<sup>2</sup> V<sup>-1</sup> s<sup>-1</sup> (Scheme 39).<sup>319</sup>

## 2.9. Borazatruxene

Truxenes in which the central benzene ring is replaced by borazine are structurally interesting systems, formally leading to hexaheterotruxenes. In 2019, Limberti *et al.* described a three-step synthesis in which **110** is converted to the corresponding borazatruxenes **111** in the presence of microwave radiation at 180 °C (Scheme 40).<sup>320</sup> The substrates enabling the synthesis of **110** are the appropriate nitriles or aldehydes. Their availability significantly increases the variety of borazatruxenes, allowing the synthesis of halogen derivatives and π-expanded systems. It should also be mentioned that the use





Scheme 40 Borazatruxene synthesis.

of appropriate aromatic ketones enables the synthesis of derivatives functionalized at the 5, 10, and 15 positions.

In the case of **111**, a clear blueshift can be observed in its absorption and emission spectra,<sup>320</sup> while its fluorescence quantum yield does not exceed 10%. Borazatruxenes are air and moisture stable and exhibit better solubility, especially in moderately polar solvents, than the practically insoluble **4**. The flat structure of heterotruxene core and strong intramolecular interactions drive columnar ordering of the molecules in the solid state, creating potential organic semiconductors.

### 3. Non-symmetrical truxenes

The non-symmetrical truxenes described in this chapter are molecules of lower symmetry (without the triple-axis). Currently, the known non-symmetrical heterotruxenes possess at least one heteroatom. When working with polycyclic condensed aromatic systems, a remarkable problem is their poor solubility. The same issue also applies to truxenes. Truxene and 5,10,15-triazatruxene can be alkylated within 5-membered rings to improve their solubility. However, this procedure cannot be used for systems containing oxygen or sulfur atoms. This obstacle is partially solved by the peripheral functionalization of the  $\pi$ -electron system with alkyl substituents. Nevertheless, this procedure prevents their further modification. Another solution to overcome their low solubility, while maintaining their unique heteroatom properties, is the concept of 5-monohetero and 5,10-diheterotruxenes (Fig. 9).

An unquestionable advantage of non-symmetrical truxenes is their solubility, resulting from *C*-alkylation. It is also worth mentioning that symmetry breaking of a molecule affects its physicochemical properties. Thus, targeted functionalization for mono-substitution is an undisputed advantage in low-symmetrical cores. However, this procedure in the case of  $C_3$ -symmetric truxenes is a challenging task.

#### 3.1. 5-Oxatruxene

5-Oxatruxene was synthesized by Górski *et al.* in 2018 during the photocyclization of the corresponding triene **113** (Scheme 41).<sup>321</sup> 5-Oxatruxene, similar to other unsubstituted truxenes, is characterized by relatively low solubility. However, the alkylation of its cyclopentadienyl rings in a basic environment significantly increases its solubility. For example, the obtained tetraethyl derivative **114** exhibits good solubility in most organic solvents. 5-Oxatruxene undergoes electrophilic substitution and

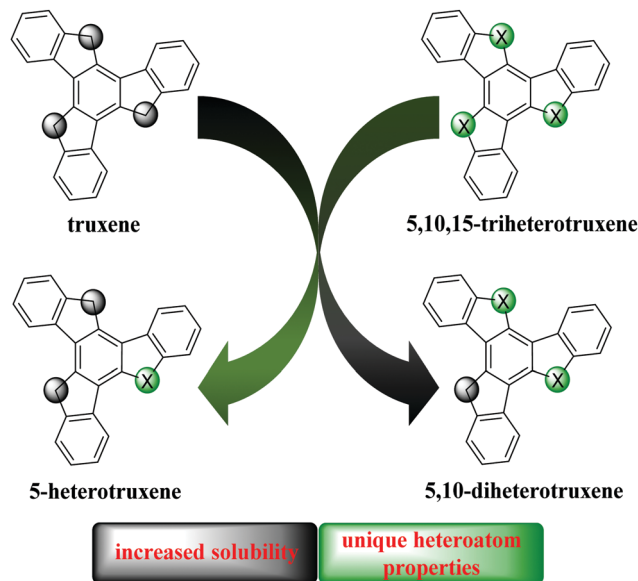
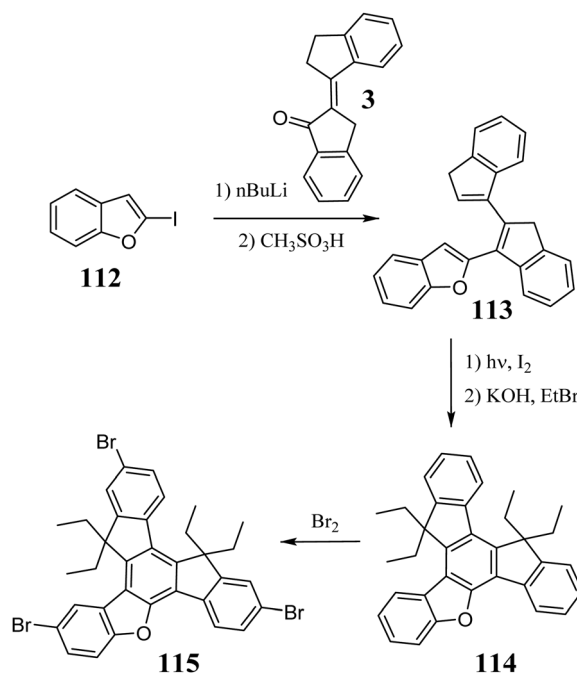


Fig. 9 Mono and diheterotruxenes as hybrids of symmetrical systems.

in excess  $\text{Br}_2$ , can be converted to the corresponding tribromo derivative **115**.<sup>125</sup>

The presence of an oxygen atom in the molecule causes structural changes, which affect the electronic levels of 5-oxatruxene. Symmetry breaking lifts the HOMO and LUMO degeneration, which is visible in the redshift in its absorption and emission spectra. Moreover, a 4-fold increase in the fluorescence quantum yield is observed.<sup>321</sup> Unlike truxene, 5-oxatruxene exhibits better thermal properties, remarkable photostability, and a reversible oxidation process.<sup>125</sup> The presence of an oxygen



Scheme 41 Synthesis and reactivity of 5-oxatruxene.

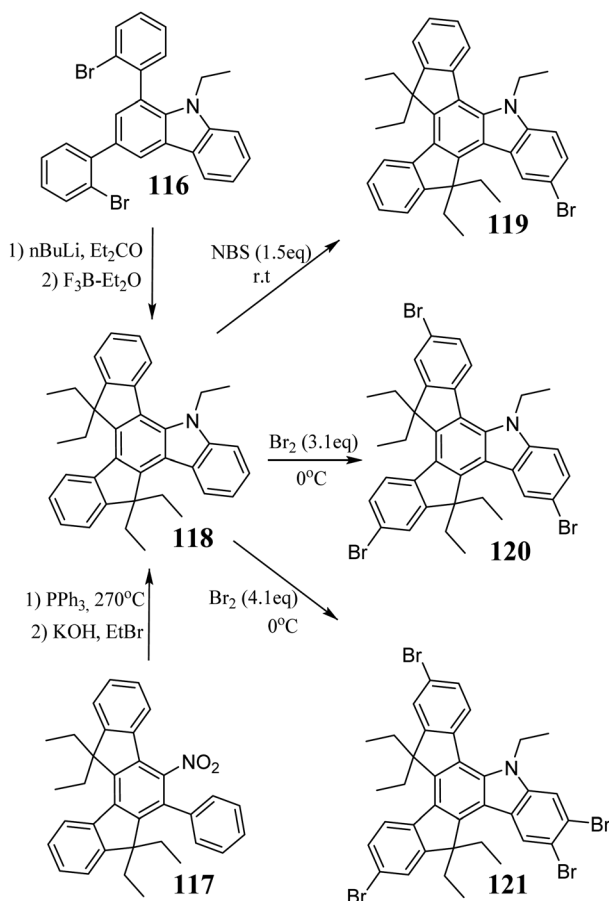


atom leads to  $\pi$ -stacking interactions, which combined with other properties, suggest its use as an HTM.

### 3.2. 5-Azatruxene

The first synthesis of the soluble 5-azatruxene **118** was described by Górski *et al.* in 2019.<sup>322</sup> **118** is a product of multistep synthesis, where the last step is the lithiation of **116**, followed by  $\text{BF}_3$ -mediated cyclodehydration (Scheme 42). An alternative method based on a solvent-free Cadogan reaction was developed one year later.<sup>125</sup> The nitro compound **117** heated with  $\text{PPh}_3$  is converted to 5-azatruxene, unprotected at the nitrogen atom. The base-promoted N–H bond ionization, followed by reaction with an alkyl halide, finally leads to the alkyl derivative **118**. The electron-rich 5-azatruxene core readily undergoes electrophilic substitution. Thus, mono- **119**,<sup>322</sup> tri- **120**, and tetrabromo derivative **121**<sup>125</sup> can be obtained in good yield.

The introduction of a nitrogen atom causes degeneration lifting and significant destabilization of the HOMO level.<sup>125</sup> Thus, among the known 5-heterotruxenes, 5-azatruxene has the most redshifted absorption and fluorescence spectra. Compared to **4**, 5-azatruxene exhibits a 4-times higher fluorescence quantum yield. Moreover, 5-azatruxene undergoes reversible oxidation, forms stable glasses, and shows the highest photostability among the known 5-heterotruxenes.



Scheme 42 Synthesis and reactivity of 5-azatruxene.

### 3.3. 5-Thiatrixene

In 2017, Maciejczyk *et al.* published a multistep synthetic protocol for 5-thiatrixene **124** (Scheme 43).<sup>323</sup> Two years later, **124** was synthesized *via* the photocyclization of **123**, clearly shortening the synthesis time.<sup>322</sup> The various 5-thiatrixene reactivity results not only from the presence of an expanded aromatic system but also from the sulfur atom. The monobromo derivative **125** can be obtained by direct lithiation of **124** and subsequent reaction with 1,2-dibromoethane.<sup>323</sup> 5-Thiatrixene readily reacts with  $\text{Br}_2$ , leading to both di- **126**<sup>323</sup> and tribromo **127**<sup>322</sup> derivatives. Interestingly, both experiments showed that the bromination process occurs first on the peripheral benzene rings away from the heterocyclic system. Due to the presence of a sulfur atom, it is possible to change its oxidation state. As a result of the reaction between 5-thiatrixene and  $\text{H}_2\text{O}_2$  or mCPBA, the corresponding sulfoxide **128** or sulfone **129** is formed.<sup>322</sup> Subsequently, the  $\text{SO}_2$  group present in **129** significantly facilitates direct *ortho* lithiation with  $\text{TMPLi}$ . Moreover, the generated organometallic derivatives undergo typical reactions with electrophiles, allowing further functionalization of the 5-thiatrixene core. The synthesis of monoiodo derivative **130** was performed using the protocol mentioned.<sup>322</sup> Oxidation of the sulfur atom changes the nature of the 5-thiatrixene core from electron-donating to electron-accepting.<sup>125</sup> Thus, D–A systems **131**–**134** can be created with 5-thiatrixene as an electron acceptor (Scheme 44).<sup>9</sup>

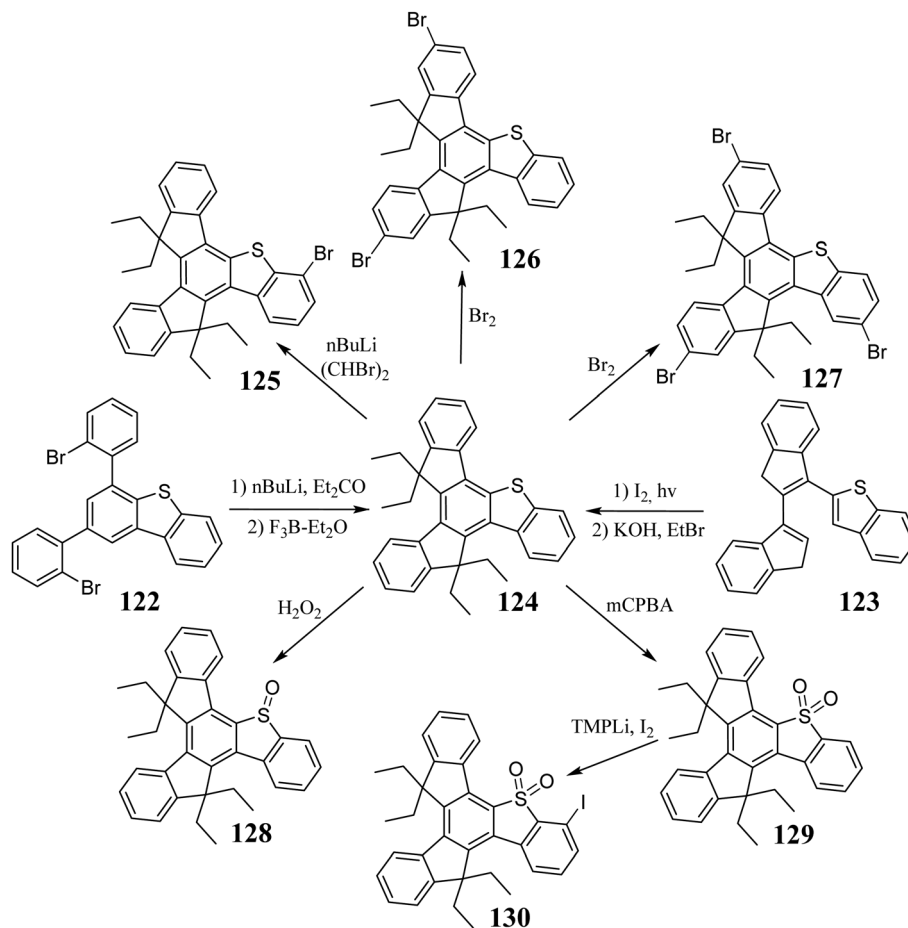
Due to the symmetry breaking in 5-thiatrixene, no degeneration of electron levels is observed.<sup>125</sup> Alternatively, the electron-donating properties of the sulfur atom cause noticeable destabilization of its HOMO level compared to **4**. Despite the symmetry breaking, a decrease in its fluorescence quantum yield is observed. The factor responsible for this is the presence of a heavy atom, increasing intersystem crossing and  $T_1$  population. The oxidation of the sulfur atom leads to sulfone **129**, which is much more stable. Moreover, the thermal properties and photostability are improved compared to **4**. 5-Thiatrixene exhibits reversible oxidation and irreversible reduction. However, in the case of the sulfone derivative, the opposite behavior is observed. 5-Thiatrixene D–A systems **131**–**134** were used as blue emissive layers in prototype OLEDs. These substances exhibited very high thermal and photostability, which directly influence the device performance, even up to  $10 \text{ kCd m}^{-2}$ , at high brightness.<sup>9</sup>

### 3.4. 5,10-Dioxatruxene

5,10-Dioxatruxene, like 5-oxatruxene, was not available synthetically for a long time. In 2020, Górski *et al.* published the multi-step synthesis of unsubstituted 5,10-dioxatruxene, in which the final reaction is the photocyclization of triene **135** (Scheme 45).<sup>324</sup> Further, basic *C*-alkylation leads to a well-soluble derivative **136**. Like other truxenes, 5,10-dioxatruxene undergoes bromination to **137**.

The introduction of two oxygen atoms in the truxene core leads to molecular symmetry breaking ( $C_{3h} \rightarrow C_s$ ); thus, no degeneration in electron structure is observed.<sup>324</sup> The described modification leads to slight destabilization of its





Scheme 43 Synthesis and reactivity of 5-thiatruxene.

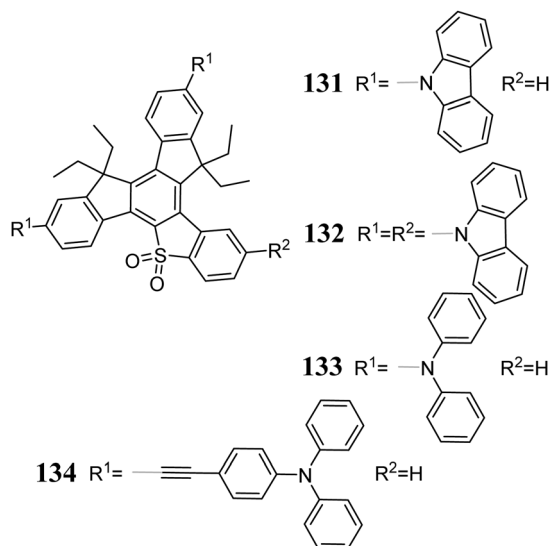
HOMO and stabilization of its LUMO compared to **4**. Thus, a redshift in its absorption and emission spectra is observed due to the decrease in HOMO–LUMO. The fluorescence quantum yield of **136** is 39.5%. The presence of oxygen atoms in the

5,10-dioxatruxene core enables effective  $\pi$ -stacking, making 5,10-dioxatruxenes promising materials for solution-processable organic semiconductors.

### 3.5. 5,10-Diazatruxene

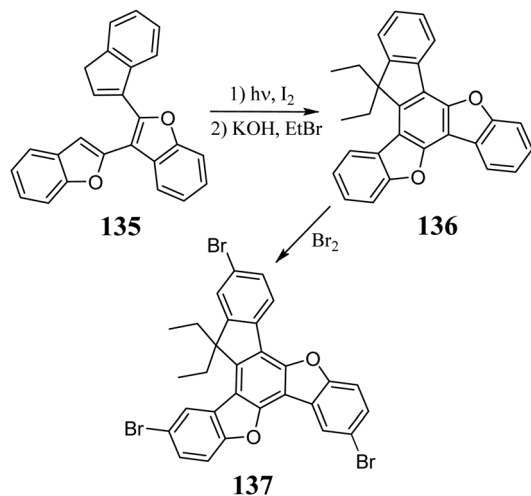
The first references to 5,10-diazatruxene appeared in the work by El Sayed *et al.* in 2017.<sup>325</sup> Consequently, the condensation of **56** was performed (Scheme 46). Subsequent studies also allowed condensation of 6-bromo<sup>326</sup> and 5-nitroindoles,<sup>327</sup> directly leading to doubly substituted 5,10-diazatruxenes. Moreover, the N-substituted indoles also undergo this reaction, allowing the direct synthesis of N-protected 5,10-diazatruxene-15-ones **140c**,<sup>324</sup> and condensation using a stoichiometric amount of MeSO<sub>3</sub>H acid in 1,2-dichloroethane.

In the presence of a base, **140a** and **b** undergo ionization, allowing reaction with various electrophiles, such as acyl chlorides,<sup>325</sup> simple alkyl halides, and more complex derivatives containing a piperidine or oxirane ring.<sup>327</sup> Alternatively, reducing the carbonyl group in **140c** by treatment with N<sub>2</sub>H<sub>4</sub> in boiling ethylene glycol makes it possible to obtain the parent 5,10-diazatruxene **142**,<sup>324</sup> which after alkylation, is transformed to the highly soluble **143** (Scheme 47). Moreover, the presence of the carbonyl group enables the reaction between **140c** and organometallic substances, leading to the appropriate 3° alcohols



Scheme 44 5-Thiatruxene-based D–A systems.

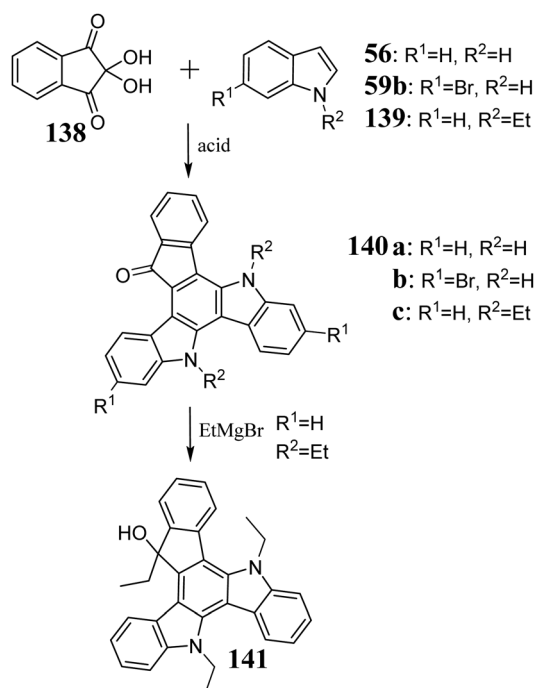




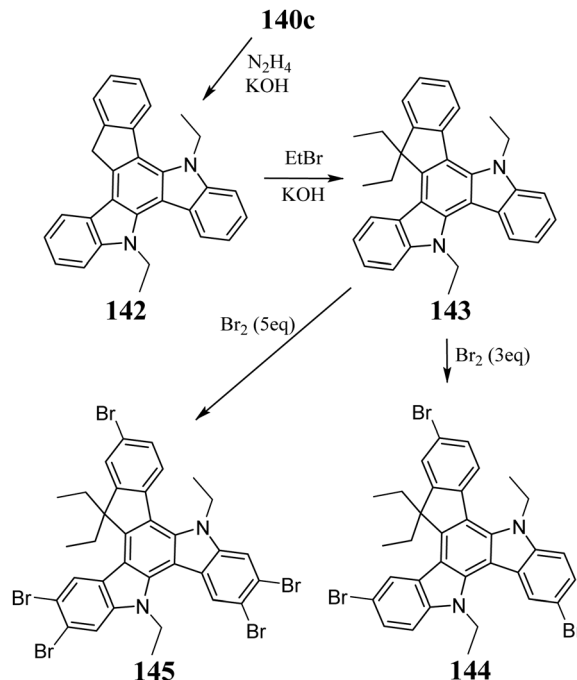
Scheme 45 Synthesis and reactivity of 5,10-dioxatruxene.

**141** (Scheme 46), significantly extending the functionalization possibilities of the 5,10-diazatruxene core.<sup>324</sup> Alternatively, **143** can be easily converted to the corresponding tri and pentabromo derivatives **144** and **145**, respectively, depending on the amount of  $\text{Br}_2$ . **140b**, **144**, and **145** are crucial derivatives in further peripheral functionalization (Scheme 47).<sup>326</sup>

The two nitrogen atoms present in the aromatic system lift the electron level degeneration, destabilize the HOMO level significantly, and increase the fluorescence quantum yield (QY = 25.5%) compared to **4**.<sup>324</sup> 5,10-Diazatruxene, like its dioxo counterpart, tends to  $\pi$ -stacking interactions. Its high HOMO energy and aggregation in the solid state suggest the possibility of using this type of substance as an HTM.



Scheme 46 Synthesis and reactivity of 5,10-diazatruxen-15-ones.

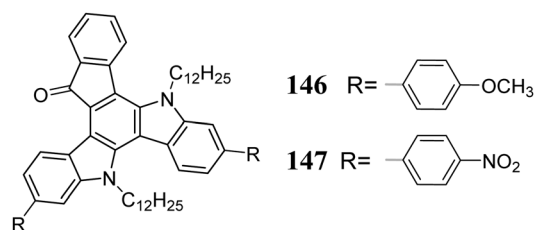


Scheme 47 Synthesis and reactivity of 5,10-diazatruxene.

Peripherally functionalized 5,10-diazatruxen-15-ones with both donor **146** and acceptor **147** substituents were employed as promising semiconductors (Scheme 48). They exhibit reversible redox processes, which combined with their high  $\pi$ -stacking in the solid state, make them potential ambipolar semiconductors.<sup>326</sup> Nevertheless, the interest in 5,10-diazatruxenes is not limited to optoelectronic applications. It has been found that the appropriate modification of the 5,10-diazatruxene core allows effective interaction with DNA, making it applicable as an anti-cancer agent.<sup>327</sup>

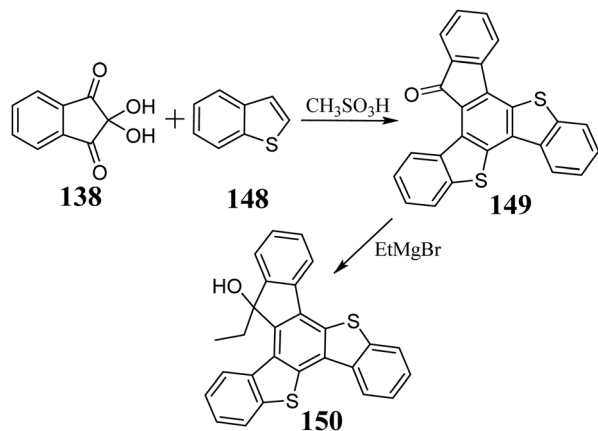
### 3.6. 5,10-Dithiatriuxene

In 2009, Suze *et al.* described the condensation between benzo[*b*]thiophene **148** and **138** in AcOH and the presence of  $\text{H}_2\text{SO}_4$ , leading to 5,10-dithiatriuxen-15-one **149**, with a yield of 68% (Scheme 49).<sup>328</sup> The same reaction can be performed using a stoichiometric amount of  $\text{MeSO}_3\text{H}$  in 1,2-dichloroethane, increasing the yield to 74%.<sup>324</sup> However, due to the negligible solubility resulting from  $\pi$ -stacking, obtaining **149** and its further functionalization are significantly impeded. Nevertheless, the reaction



Scheme 48 5,10-Diazatruxene-15-one-based D-A ambipolar semiconductors.



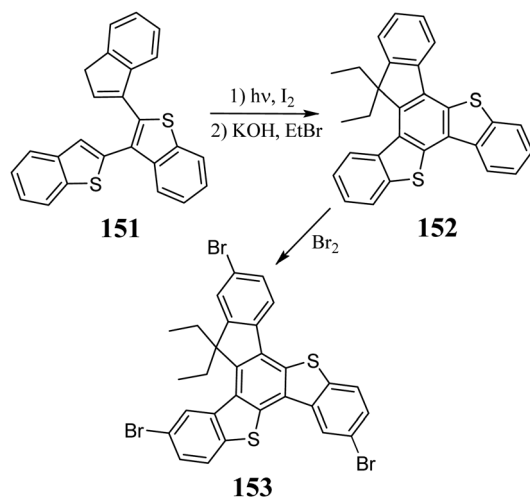


Scheme 49 Synthesis and reactivity of 5,10-dithiatruxene-15-one.

between **149** and organometallic reagents, leading to soluble 3° alcohol **150**, is possible.<sup>324</sup>

The soluble 5,10-dithiatruxene **152** was synthesized for the first time in 2020 by Górski *et al.* **151**, in the presence of a catalytic amount of I<sub>2</sub> and UV light, undergoes photocyclization to unsubstituted 5,10-dithiatruxene (Scheme 50). After C-alkylation, within a carbocyclic five-membered ring, its solubility significantly increases. By treating **152** with excess Br<sub>2</sub>, the appropriate bromo derivative **153** is obtained, with nearly quantitative yield.

The HOMO level of 5,10-dithiatruxene is destabilized compared to **4**.<sup>324</sup> Due to the low symmetry of the molecule, the degeneration of its electron levels is lifted. However, despite the electron transitions being allowed, 5,10-dithiatruxene has a relatively low fluorescence quantum yield. The ability to exhibit strong  $\pi$ -stacking interactions in the solid state, characteristic for 5,10-diheterotruxenes, is also observed in the case of **149** and **152**. Therefore, 5,10-dithiatruxenes should be considered as potential organic semiconductors.



Scheme 50 Synthesis and reactivity of 5,10-dithiatruxene.

## 4. Conclusion

The present review summarized the knowledge on the synthesis and physicochemistry of (hetero)truxenes up to 2021, including their synthesis, reactivity, spectral, and redox properties. The parent heptacyclic, star-shaped hydrocarbon, can be modified towards the desired properties by either heteroatom displacement or peripheral functionalization. The presence of C<sub>3</sub> symmetry significantly influences every aspect mentioned. To attract a broader group of readers, the physicochemical properties of (hetero)truxenes together with their potential applications were discussed. The ease of heterotruxene functionalization allows fitting physicochemical properties and constructing macromolecules, COFs, and MOFs. We highlighted the difficulties in synthesizing heteroanalogues and their different reactivity. Multiple citations next to each subsection allow the choice of a suitable synthetic path. This review is expected to be helpful for both synthetic and material chemists.

## Conflicts of interest

There are no conflicts to declare.

## Acknowledgements

This work was supported by National Science Centre (grant no. FUGA 4, 2015/16/S/ST4/00427) and in part by the Institute of Physical Chemistry, Polish Academy of Sciences.

## References

- X. C. Li, C. Y. Wang, W. Y. Lai and W. Huang, *J. Mater. Chem. C*, 2016, **4**, 10574–10587.
- M. T. El Sayed, *J. Heterocycl. Chem.*, 2018, **55**, 21–43.
- K. Shi, J. Y. Wang and J. Pei, *Chem. Rec.*, 2015, **15**, 52–78.
- F. Goubard and F. Dumur, *RSC Adv.*, 2015, **5**, 3521–3551.
- S. A. Wagay, I. A. Rather and R. Ali, *ChemistrySelect*, 2019, **4**, 12272–12288.
- C. Yao, Y. Yu, X. Yang, H. Zhang, Z. Huang, X. Xu, G. Zhou, L. Yue and Z. Wu, *J. Mater. Chem. C*, 2015, **3**, 5783–5794.
- Y. Liu, Y. Chen, H. Li, S. Wang, X. Wu, H. Tong and L. Wang, *ACS Appl. Mater. Interfaces*, 2020, **12**, 30652–30658.
- P. L. dos Santos, J. S. Ward, D. G. Congrave, A. S. Batsanov, J. Eng, J. E. Stacey, T. J. Penfold, A. P. Monkman and M. R. Bryce, *Adv. Sci.*, 2018, **5**, 1700989 (1–9).
- M. R. Maciejczyk, S. Zhang, G. J. Hedley, N. Robertson, I. D. W. Samuel and M. Pietraszkiewicz, *Adv. Funct. Mater.*, 2019, **1807572**, 1–13.
- C. Ruiz, I. Arrechea-Marcos, A. Benito-Hernández, E. Gutiérrez-Puebla, M. Á. Monge, J. T. López Navarrete, M. C. Ruiz Delgado, R. P. Ortiz and B. Gómez-Lor, *J. Mater. Chem. C*, 2018, **6**, 50–56.
- Y. Sun, K. Xiao, Y. Liu, J. Wang, J. Pei, G. Yu and D. Zhu, *Adv. Funct. Mater.*, 2005, **15**, 818–822.



- 12 S. Mula, T. Han, T. Heiser, P. L  v  que, N. Leclerc, A. P. Srivastava, A. Ruiz-Carretero and G. Ulrich, *Chem. – Eur. J.*, 2019, **25**, 8304–8312.
- 13 B. Pan, Y.-Z. Zhu, D. Ye, F. Li, Y.-F. Guo and J.-Y. Zheng, *New J. Chem.*, 2018, **42**, 4133–4141.
- 14 L. Zhang, X. Yang, W. Wang, G. G. Gurzadyan, J. Li, X. Li, J. An, Z. Yu, H. Wang, B. Cai, A. Hagfeldt and L. Sun, *ACS Energy Lett.*, 2019, **4**, 943–951.
- 15 L. Miu, S. Yan, H. Yao, Q. Chen, J. Zhang, Z. Wang, P. Cai, T. Hu, S. Ding, J. Chen, M. Liang and S. Yang, *Dyes Pigm.*, 2019, **168**, 1–11.
- 16 L. Wang, Q. Fang, Q. Lu, S.-J. Zhang, Y.-Y. Jin and Z.-Q. Liu, *Org. Lett.*, 2015, **17**, 4164–4167.
- 17 C. K. M. Chan, C.-H. Tao, H.-L. Tam, N. Zhu, V. W.-W. Yam and K.-W. Cheah, *Inorg. Chem.*, 2009, **48**, 2855–2864.
- 18 J. Shao, Z. Guan, Y. Yan, C. Jiao, Q.-H. Xu and C. Chi, *J. Org. Chem.*, 2011, **76**, 780–790.
- 19 G. He, J. Shao, Y. Li, J. Hu, H. Zhu, X. Wang, Q. Guo, C. Chi and A. Xia, *Phys. Chem. Chem. Phys.*, 2016, **18**, 6789–6798.
- 20 Y. Nailwal, A. D. D. Wonanke, M. A. Addicoat and S. K. Pal, *Macromolecules*, 2021, **54**, 6595–6604.
- 21 K.-R. Wang, Y.-Q. Wang, H.-W. An, J.-C. Zhang and X.-L. Li, *Chem. – Eur. J.*, 2013, **19**, 2903–2909.
- 22 L. K. Macreadie, R. Babarao, C. J. Setter, S. J. Lee, O. T. Qazvini, A. J. Seeber, J. Tsanaksidis, S. G. Telfer, S. R. Batten and M. R. Hill, *Angew. Chem., Int. Ed.*, 2020, **59**, 6090–6098.
- 23 L. Yang, Y. Ma, Y. Xu and G. Chang, *Chem. Commun.*, 2019, **55**, 11227–11230.
- 24 L. Yang, W. Wei, Y. Ma, Y. Xu and G. Chang, *J. Power Sources*, 2020, **449**, 227551.
- 25 G. W. Kim, R. Lampande, D. C. Choe, H. W. Bae and J. H. Kwon, *Thin Solid Films*, 2015, **589**, 105–110.
- 26 X. Yang, D. Zhang, Y. Liao and D. Zhao, *J. Org. Chem.*, 2020, **85**, 5761–5770.
- 27 T. Kirschbaum, F. Rominger and M. Mastalerz, *Angew. Chem., Int. Ed.*, 2020, **59**, 270–274.
- 28 R. Dorel and A. M. Echavarren, *Acc. Chem. Res.*, 2019, **52**, 1812–1823.
- 29 X. Wang, P. Peng, W. Xuan, Y. Wang, Y. Zhuang, Z. Tian and X. Cao, *Org. Biomol. Chem.*, 2018, **16**, 34–37.
- 30 J. Zhu, D. Zhang, T. K. Ronson, W. Wang, L. Xu, H. Yang and J. R. Nitschke, *Angew. Chem., Int. Ed.*, 2021, 11789–11792.
- 31 M. Yamashina, Y. Tanaka, R. Lavendomme, T. K. Ronson, M. Pittelkow and J. R. Nitschke, *Nature*, 2019, **574**, 511–515.
- 32 X. Yang, S. Huang, M. Ortiz, X. Wang, Y. Cao, O. Kareem, Y. Jin, F. Huang, X. Wang and W. Zhang, *Org. Chem. Front.*, 2021, **8**, 4723–4729.
- 33 M. M. Boorum and L. T. Scott, *Modern Arene Chemistry*, Wiley-VCH Verlag GmbH & Co. KGaA, Weinheim, FRG, 2002, pp. 20–31.
- 34 G. Metz, *Synthesis*, 1972, 614–615.
- 35 E. V. Dehmlow and T. Kelle, *Synth. Commun.*, 1997, **27**, 2021–2031.
- 36 T. W. Warmerdam, R. J. M. Nolte, W. Drenth, J. C. Van Miltenburg, D. Frenkel and R. J. J. Zijlstra, *Liq. Cryst.*, 1988, **3**, 1087–1104.
- 37 B. G  mez-Lor,   . de Frutos, P. A. Ceballos, T. Granier and A. M. Echavarren, *Eur. J. Org. Chem.*, 2001, 2107–2114.
- 38 A. W. Amick and L. T. Scott, *J. Org. Chem.*, 2007, **72**, 3412–3418.
- 39 GB 2520791 A, 2015.
- 40 H. Terai, H. Takaya and T. Naota, *Tetrahedron Lett.*, 2006, **47**, 1705–1708.
- 41 J.-B. Chen, C. Zhou, R.-Q. Lu, X.-C. Wang, H. Qu, M. Saha, H.-L. Liu, H. Zhang and X.-Y. Cao, *Chem. – Eur. J.*, 2019, **25**, 1293–1299.
- 42 S. S. Elmorsy, A. Pelter, K. Smith, M. B. Hursthouse and D. Ando, *Tetrahedron Lett.*, 1992, **33**, 821–824.
- 43 H. Isla, B. Grimm, E. M. P  rez, M. Rosario Torres, M.   ngeles Herranz, R. Viruela, J. Arag  , E. Ort  , D. M. Guldi and N. Mart  n, *Chem. Sci.*, 2012, **3**, 498–508.
- 44 L. Sanguinet, J. C. Williams, Z. Yang, R. J. Twieg, G. Mao, K. D. Singer, G. Wiggers and R. G. Petschek, *Chem. Mater.*, 2006, **18**, 4259–4269.
- 45 Y. N. Oded and I. Agranat, *Tetrahedron Lett.*, 2014, **55**, 636–638.
- 46 X. Zhang, X. Ji, R. Su, B. L. Weeks, Z. Zhang and S. Deng, *ChemPlusChem*, 2013, **78**, 703–711.
- 47 G. Zhang, V. Lami, F. Rominger, Y. Vaynzof and M. Mastalerz, *Angew. Chemie*, 2016, **128**, 4045–4049.
- 48 J.-Y. Wang, J. Yan, L. Ding, Y. Ma and J. Pei, *Adv. Funct. Mater.*, 2009, **19**, 1746–1752.
- 49 H. Jiang, N. Lai, J. Tang, X. Tian, F. Wei, W. Bai and Y. Xu, *J. Photochem. Photobiol., A*, 2019, **369**, 195–201.
- 50 D. Raksasorn, S. Namuangruk, N. Prachumrak, T. Sudyoasuk, V. Promarak, M. Sukwattanasinitt and P. Rashatasakhon, *RSC Adv.*, 2015, **5**, 72841–72848.
- 51 T. L. Tisch, T. J. Lynch and R. Dominguez, *J. Organomet. Chem.*, 1989, **377**, 265–273.
- 52   . de Frutos, B. G  mez-Lor, T. Granier, M.   . Monge, E. Guti  rrez-Puebla and A. M. Echavarren, *Angew. Chem., Int. Ed.*, 1999, **38**, 204–207.
- 53 H. Satoh, G. Yamamoto and Y. Mazaki, *Bull. Chem. Soc. Jpn.*, 2006, **79**, 938–943.
- 54 D. K. Frantz, J. J. Walish and T. M. Swager, *Org. Lett.*, 2013, **15**, 4782–4785.
- 55 K. Isoda, T. Yasuda and T. Kato, *Chem. – Asian J.*, 2009, **4**, 1619–1625.
- 56 E. M. P  rez, M. Sierra, L. S  nchez, M. R. Torres, R. Viruela, P. M. Viruela, E. Ort   and N. Mart  n, *Angew. Chem., Int. Ed.*, 2007, **46**, 1847–1851.
- 57 M. Kimura, S. Kuwano, Y. Sawaki, H. Fujikawa, K. Noda, Y. Taga and K. Takagi, *J. Mater. Chem.*, 2005, **15**, 2393–2398.
- 58 M. Ruiz, B. G  mez-Lor, A. Santos and A. M. Echavarren, *Eur. J. Org. Chem.*, 2004, 858–866.
- 59 S. Kotha, R. Ali, N. R. Panguluri, A. Datta and K. K. Kannaujiya, *Tetrahedron Lett.*, 2018, **59**, 4080–4085.
- 60 M.-T. Kao, J.-H. Chen, Y.-Y. Chu, K.-P. Tseng, C.-H. Hsu, K.-T. Wong, C.-W. Chang, C.-P. Hsu and Y.-H. Liu, *Org. Lett.*, 2011, **13**, 1714–1717.



- 61 X.-Y. Cao, W.-B. Zhang, J.-L. Wang, X.-H. Zhou, H. Lu and J. Pei, *J. Am. Chem. Soc.*, 2003, **125**, 12430–12431.
- 62 X.-Y. Cao, X.-H. Liu, X.-H. Zhou, Y. Zhang, Y. Jiang, Y. Cao, Y.-X. Cui and J. Pei, *J. Org. Chem.*, 2004, **69**, 6050–6058.
- 63 L. Liu and S. G. Telfer, *J. Am. Chem. Soc.*, 2015, **137**, 3901–3909.
- 64 T.-C. Lin, B.-K. Tsai, T.-Y. Huang, W. Chien, Y.-Y. Liu, M.-H. Li and M.-Y. Tsai, *Dyes Pigm.*, 2015, **120**, 99–111.
- 65 K. Lin, S. Wang, Z. Wang, Q. Yin, X. Liu, J. Jia, X. Jia, P. Luo, X. Jiang, C. Duan, F. Huang and Y. Cao, *Front. Chem.*, 2018, **6**, 328.
- 66 M. Tasiar, O. Vakuliuk, D. Koga, B. Koszarna, K. Górski, M. Grzybowski, Ł. Kielesiński, M. Krzeszewski and D. T. Gryko, *J. Org. Chem.*, 2020, **85**, 13529–13543.
- 67 M. Sen Yuan, Q. Fang, Y. R. Zhang and Q. Wang, *Spectrochim. Acta, Part A*, 2011, **79**, 1112–1115.
- 68 H.-W. Wen and P.-C. Yang, *RSC Adv.*, 2016, **6**, 60308–60317.
- 69 X.-Y. Cao, X.-H. Zhou, H. Zi and J. Pei, *Macromolecules*, 2004, **37**, 8874–8882.
- 70 W.-Y. Lai, Q.-Y. He, Z. Ma and W. Huang, *Chem. Lett.*, 2009, **38**, 286–287.
- 71 X.-Y. Cao, W. Zhang, H. Zi and J. Pei, *Org. Lett.*, 2004, **6**, 4845–4848.
- 72 S. Diring and R. Ziessel, *Tetrahedron Lett.*, 2009, **50**, 1203–1208.
- 73 X. Yang, Q. Zheng, C. Tang, D. Cai, S.-C. Chen and Y. Ma, *Dyes Pigm.*, 2013, **99**, 366–373.
- 74 X. Xu, D. Sun, J. Yang, G. Zhu, Y. Fang, C. P. Gros, F. Bolze and H.-J. Xu, *Dyes Pigm.*, 2020, **179**, 108380.
- 75 J. Yang, F.-J. Cai, X.-M. Yuan, T. Meng, G.-X. Xin, S.-F. Wang, C. P. Gros and H.-J. Xu, *J. Porphyr. Phthalocyanines*, 2018, **22**, 777–783.
- 76 Y. Kim, S. Das, S. Bhattacharya, S. Hong, M. G. Kim, M. Yoon, S. Natarajan and K. Kim, *Chem. – Eur. J.*, 2012, **18**, 16642–16648.
- 77 J. Yang, H. Jiang, N. Desbois, G. Zhu, C. P. Gros, Y. Fang, F. Bolze, S. Wang and H.-J. Xu, *Dyes Pigm.*, 2020, **176**, 108183.
- 78 Y. Wang, H. Fang, I. Tranca, H. Qu, X. Wang, A. J. Markvoort, Z. Tian and X. Cao, *Nat. Commun.*, 2018, **9**, 488.
- 79 B. Du, D. Fortin and P. D. Harvey, *Inorg. Chem.*, 2011, **50**, 11493–11505.
- 80 Y. Wu, X. Hao, J. Wu, J. Jin and X. Ba, *Macromolecules*, 2010, **43**, 731–738.
- 81 G. Zhang, F. Rominger and M. Mastalerz, *Chem. – Eur. J.*, 2016, **22**, 3084–3093.
- 82 L. Zhao, W. Wang and M.-S. Yuan, *Spectrochim. Acta, Part A*, 2015, **135**, 63–68.
- 83 F. Li, B. Zhao, Y. Chen, Y. Zhang, T. Wang and S. Xue, *Spectrochim. Acta, Part A*, 2017, **185**, 20–26.
- 84 B. Kaur, S. Karuthedath, C. S. P. De Castro, F. Laquai and J. Jacob, *ChemistrySelect*, 2020, **5**, 109–116.
- 85 H. Tsuji, Y. Ota, S. Furukawa, C. Mitsui, Y. Sato and E. Nakamura, *Asian J. Org. Chem.*, 2012, **1**, 34–37.
- 86 M.-Y. Wang, Q.-J. Zhang, Q.-Q. Shen, Q.-Y. Li and S.-J. Ren, *Chin. J. Polym. Sci.*, 2020, **38**, 151–157.
- 87 E. Aktas, J. Jiménez-López, C. Rodríguez-Seco, R. Pudi, M. A. Ortuño, N. López and E. Palomares, *ChemPhysChem*, 2019, **20**, 2702–2711.
- 88 Y. Che, X. Yuan, F. Cai, J. Zhao, X. Zhao, H. Xu and L. Liu, *Dyes Pigm.*, 2019, **171**, 107756.
- 89 M. Pfeiffermann, R. Dong, R. Graf, W. Zajaczkowski, T. Gorelik, W. Pisula, A. Narita, K. Müllen and X. Feng, *J. Am. Chem. Soc.*, 2015, **137**, 14525–14532.
- 90 W.-Y. Lai, D. Liu and W. Huang, *Macromol. Chem. Phys.*, 2011, **212**, 445–454.
- 91 K. M. Choi, K.-Y. Kim, T.-D. Kim, R. R. Das, B. K. Choi, J. J. Park, J.-M. Kim and K.-S. Lee, *J. Nanosci. Nanotechnol.*, 2010, **10**, 6916–6919.
- 92 J. Huang, B. Xu, J. H. Su, C. H. Chen and H. Tian, *Tetrahedron*, 2010, **66**, 7577–7582.
- 93 Y. Xie, X. Zhang, Y. Xiao, Y. Zhang, F. Zhou, J. Qi and J. Qu, *Chem. Commun.*, 2012, **48**, 4338–4340.
- 94 X. Zhang, H. Song, J. Xiao, T. Ren, S. Wang, Z. Liu, X. Ba and Y. Wu, *Aust. J. Chem.*, 2015, **68**, 505–512.
- 95 R. Sharma, D. Volyniuk, C. Popli, O. Bezikonny, J. V. Grazulevicius and R. Misra, *J. Phys. Chem. C*, 2018, **122**, 15614–15624.
- 96 C. Tang, X.-D. Liu, F. Liu, X.-L. Wang, H. Xu, R.-L. Liu, Z. Rong and W. Huang, *J. Chem. Res.*, 2013, **37**, 242–247.
- 97 X.-F. Duan, J.-L. Wang and J. Pei, *Org. Lett.*, 2005, **7**, 4071–4074.
- 98 X. Wen, D. Zhang, T. Ren, J. Xiao, Y. Wu, L. Bai and X. Ba, *Dyes Pigm.*, 2017, **137**, 437–444.
- 99 Y.-D. Jiu, C.-F. Liu, J.-Y. Wang, W.-Y. Lai, Y. Jiang, W.-D. Xu, X.-W. Zhang and W. Huang, *Polym. Chem.*, 2015, **6**, 8019–8028.
- 100 Y. Fan, Q. Wen, T.-G. Zhan, Q.-Y. Qi, J.-Q. Xu and X. Zhao, *Chem. – Eur. J.*, 2017, **23**, 5668–5672.
- 101 Q. Zhang, C. Zhang, L. Cao, Z. Wang, B. An, Z. Lin, R. Huang, Z. Zhang, C. Wang and W. Lin, *J. Am. Chem. Soc.*, 2016, **138**, 5308–5315.
- 102 W.-Y. Lai, R. Xia, D. D. C. Bradley and W. Huang, *Chem. – Eur. J.*, 2010, **16**, 8471–8479.
- 103 Y. Jiang, Y.-X. Lu, Y.-X. Cui, Q.-F. Zhou, Y. Ma and J. Pei, *Org. Lett.*, 2007, **9**, 4539–4542.
- 104 J.-M. Koenen, S. Jung, A. Patra, A. Helfer and U. Scherf, *Adv. Mater.*, 2012, **24**, 681–686.
- 105 Q.-Q. Chen, F. Liu, Z. Ma, B. Peng, W. Wei and W. Huang, *Synlett*, 2007, 3145–3148.
- 106 X.-Y. Cao, H. Zi, W. Zhang, H. Lu and J. Pei, *J. Org. Chem.*, 2005, **70**, 3645–3653.
- 107 R. Sharma, R. Maragani and R. Misra, *New J. Chem.*, 2018, **42**, 882–890.
- 108 R. Misra, R. Sharma and S. M. Mobin, *Dalton Trans.*, 2014, **43**, 6891–6896.
- 109 R. Sharma, M. B. Thomas, R. Misra and F. D'Souza, *Angew. Chem., Int. Ed.*, 2019, **58**, 4350–4355.
- 110 S. Diring, F. Puntoriero, F. Nastasi, S. Campagna and R. Ziessel, *J. Am. Chem. Soc.*, 2009, **131**, 6108–6110.
- 111 J.-L. Wang, X.-F. Duan, B. Jiang, L.-B. Gan, J. Pei, C. He and Y.-F. Li, *J. Org. Chem.*, 2006, **71**, 4400–4410.





- 112 B. Ventura, A. Barbieri, F. Barigelletti, S. Diring and R. Ziessel, *Inorg. Chem.*, 2010, **49**, 8333–8346.
- 113 J.-L. Wang, Y.-T. Chan, C. N. Moorefield, J. Pei, D. A. Modarelli, N. C. Romano and G. R. Newkome, *Macromol. Rapid Commun.*, 2010, **31**, 850–855.
- 114 S. Diring, R. Ziessel, F. Barigelletti, A. Barbieri and B. Ventura, *Chem. – Eur. J.*, 2010, **16**, 9226–9236.
- 115 C. K. M. Chan, C.-H. Tao, K. F. Li, K. Man-Chung Wong, N. Zhu, K.-W. Cheah and V. W. W. Yam, *J. Organomet. Chem.*, 2011, **696**, 1163–1173.
- 116 C. Po, C.-H. Tao, K.-F. Li, C. K. M. Chan, H. L.-K. Fu, K.-W. Cheah and V. W.-W. Yam, *Inorg. Chim. Acta*, 2019, **488**, 214–218.
- 117 H. Norouzi-Arasi, A. K. Pal, S. Nag, D. Chartrand and G. S. Hanan, *Chem. Commun.*, 2016, **52**, 12159–12162.
- 118 R. Dorel, P. de Mendoza, P. Calleja, S. Pascual, E. González-Cantalapiedra, N. Cabello and A. M. Echavarren, *Eur. J. Org. Chem.*, 2016, 3171–3176.
- 119 B. Gómez-Lor, Ó. de Frutos, A. M. Echavarren and B. Gómez-Lor, *Chem. Commun.*, 1999, 2431–2432.
- 120 K. Y. Amsharov, N. Abdurakhmanova, S. Stepanow, S. Rauschenbach, M. Jansen and K. Kern, *Angew. Chem., Int. Ed.*, 2010, **49**, 9392–9396.
- 121 K. Y. Amsharov and M. Jansen, *Chem. Commun.*, 2009, 2691–2693.
- 122 A. Mueller and K. Y. Amsharov, *Eur. J. Org. Chem.*, 2012, 6155–6164.
- 123 D. Baunsgaard, N. Harrit, M. El Balsami, F. Negri, G. Orlandi, J. Frederiksen and R. Wilbrandt, *J. Phys. Chem. A*, 1998, **102**, 10007–10016.
- 124 T. Ogaki, E. Ohta, Y. Oda, H. Sato, Y. Matsui, M. Kumeda and H. Ikeda, *Asian J. Org. Chem.*, 2017, **6**, 290–296.
- 125 K. Górski, K. Noworyta and J. Mech-Piskorz, *RSC Adv.*, 2020, **10**, 42363–42377.
- 126 R. Wang, K. Jiang, H. Yu, F. Wu, L. Zhu and H. Yan, *Mater. Chem. Front.*, 2019, **3**, 2137–2142.
- 127 T. H. Nguyen, J. Malthete and C. Destrade, *Mol. Cryst. Liq. Cryst.*, 1981, **64**, 291–298.
- 128 J. M. Buisine, R. Cayuela, C. Destrade and N. H. Tinh, *Mol. Cryst. Liq. Cryst.*, 1987, **144**, 137–160.
- 129 C. Destrade, P. Foucher, J. Malthete and T. H. Nguyen, *Phys. Lett.*, 1982, **88**, 187–190.
- 130 J. Lejay and M. Pesquer, *Mol. Cryst. Liq. Cryst.*, 1983, **95**, 31–43.
- 131 J. Lejay and M. Pesquer, *Mol. Cryst. Liq. Cryst.*, 1984, **111**, 293–310.
- 132 C. Destrade, H. Gasparoux, A. Babeau, N. Huu Tinh and J. Malthete, *Mol. Cryst. Liq. Cryst.*, 1981, **67**, 37–47.
- 133 S. Gómez-Esteban, A. Benito-Hernandez, R. Termine, G. Hennrich, J. T. L. Navarrete, M. C. Ruiz Delgado, A. Golemme and B. Gómez-Lor, *Chem. – Eur. J.*, 2018, **24**, 3576–3583.
- 134 D. R. Vinayakumara, M. Kumar, P. Sreekanth, R. Philip and S. Kumar, *RSC Adv.*, 2015, **5**, 26596–26603.
- 135 W.-B. Zhang, W.-H. Jin, X.-H. Zhou and J. Pei, *Tetrahedron*, 2007, **63**, 2907–2914.
- 136 J. Pei, J.-L. Wang, X.-Y. Cao, X.-H. Zhou and W.-B. Zhang, *J. Am. Chem. Soc.*, 2003, **125**, 9944–9945.
- 137 J.-L. Wang, J. Luo, L.-H. Liu, Q.-F. Zhou, Y. Ma and J. Pei, *Org. Lett.*, 2006, **8**, 2281–2284.
- 138 A. L. Kanibolotsky, R. Berridge, P. J. Skabara, I. F. Perepichka, D. D. C. Bradley and M. Koeberg, *J. Am. Chem. Soc.*, 2004, **126**, 13695–13702.
- 139 Q.-Q. Chen, F. Liu, Z. Ma, B. Peng, W. Wei and W. Huang, *Chem. Lett.*, 2008, **37**, 178–179.
- 140 Y. Jiang, J.-Y. Wang, Y. Ma, Y.-X. Cui, Q.-F. Zhou and J. Pei, *Org. Lett.*, 2006, **8**, 4287–4290.
- 141 N. A. Montgomery, J.-C. Denis, S. Schumacher, A. Ruseckas, P. J. Skabara, A. L. Kanibolotsky, M. J. Paterson, I. Galbraith, G. A. Turnbull and I. D. W. Samuel, *J. Phys. Chem. A*, 2011, **115**, 2913–2919.
- 142 M. M. Oliva, J. Casado, J. T. López Navarrete, R. Berridge, P. J. Skabara, A. L. Kanibolotsky and I. F. Perepichka, *J. Phys. Chem. B*, 2007, **111**, 4026–4035.
- 143 K. M. Omer, A. L. Kanibolotsky, P. J. Skabara, I. F. Perepichka and A. J. Bard, *J. Phys. Chem. B*, 2007, **111**, 6612–6619.
- 144 Z. Mohsan, A. L. Kanibolotsky, A. J. Stewart, A. R. Inigo, L. Dennany and P. J. Skabara, *J. Mater. Chem. C*, 2015, **3**, 1166–1171.
- 145 M. Wu, Z. Gong, A. J. C. Kuehne, A. L. Kanibolotsky, Y. J. Chen, I. F. Perepichka, A. R. Mackintosh, E. Gu, P. J. Skabara, R. A. Pethrick and M. D. Dawson, *Opt. Express*, 2009, **17**, 16436–16443.
- 146 J. L. Wang, Z. He, H. Wu, H. Cui, Y. Li, Q. Gong, Y. Cao and J. Pei, *Chem. – Asian J.*, 2010, **5**, 1455–1465.
- 147 S. C. Yuan, Q. Sun, T. Lei, B. Du, Y. F. Li and J. Pei, *Tetrahedron*, 2009, **65**, 4165–4172.
- 148 J.-L. Wang, J. Yan, Z.-M. Tang, Q. Xiao, Y. Ma and J. Pei, *J. Am. Chem. Soc.*, 2008, **130**, 9952–9962.
- 149 J.-L. Wang, Z.-M. Tang, Q. Xiao, Y. Ma and J. Pei, *Org. Lett.*, 2009, **11**, 863–866.
- 150 C. R. Belton, A. L. Kanibolotsky, J. Kirkpatrick, C. Orofino, S. E. T. Elmasly, P. N. Stavrinou, P. J. Skabara and D. D. C. Bradley, *Adv. Funct. Mater.*, 2013, **23**, 2792–2804.
- 151 Y. Wang, G. Tsiminis, Y. Yang, A. Ruseckas, A. L. Kanibolotsky, I. F. Perepichka, P. J. Skabara, G. A. Turnbull and I. D. W. Samuel, *Synth. Met.*, 2010, **160**, 1397–1400.
- 152 C. Liu, T. Lu, W. Lai and W. Huang, *Chem. – Asian J.*, 2019, **14**, 3442–3448.
- 153 W. Xu, J. Yi, W.-Y. Lai, L. Zhao, Q. Zhang, W. Hu, X.-W. Zhang, Y. Jiang, L. Liu and W. Huang, *Adv. Funct. Mater.*, 2015, **25**, 4617–4625.
- 154 CN 107445849 A, 2017, 1–20.
- 155 H. Zhang, X. Liu, T. Lu, P. Lv and W. Lai, *Chem. – Eur. J.*, 2019, **25**, 3909–3917.
- 156 B. Guzelurk, A. L. Kanibolotsky, C. Orofino-Pena, N. Laurand, M. D. Dawson, P. J. Skabara and H. V. Demir, *J. Mater. Chem. C*, 2015, **3**, 12018–12025.
- 157 H. Zhou, X. Zhao, T. Huang, R. Lu, H. Zhang, X. Qi, P. Xue, X. Liu and X. Zhang, *Org. Biomol. Chem.*, 2011, **9**, 1600–1607.



- 158 X. Zhou, J.-K. Feng and A.-M. Ren, *Synth. Met.*, 2005, **155**, 615–617.
- 159 Q. Lv, S. Feng, L. Jing, Q. Zhang, M. Qi, J. Wang, H. Bai and R. Fu, *J. Chromatogr. A*, 2016, **1454**, 114–119.
- 160 Q. Zhang, M. Qi and J. Wang, *J. Chromatogr. A*, 2017, **1525**, 152–160.
- 161 Y. Yang, M. Qi and J. Wang, *J. Chromatogr. A*, 2018, **1578**, 67–75.
- 162 M. Wang, Y. Yang, M. Qi and J. Wang, *RSC Adv.*, 2017, **7**, 44665–44672.
- 163 C. Cheng, Y. Jiang, C.-F. Liu, J.-D. Zhang, W.-Y. Lai and W. Huang, *Chem. – Asian J.*, 2016, **11**, 3589–3597.
- 164 J. Wang, Y. Chen, M. Liang, G. Ge, R. Zhou, Z. Sun and S. Xue, *Dyes Pigm.*, 2016, **125**, 399–406.
- 165 L. Guan, X. Yin, D. Zhao, C. Wang, Q. An, J. Yu, N. Shrestha, C. R. Grice, R. A. Awni, Y. Yu, Z. Song, J. Zhou, W. Meng, F. Zhang, R. J. Ellingson, J. Wang, W. Tang and Y. Yan, *J. Mater. Chem. A*, 2017, **5**, 23319–23327.
- 166 CN 107353891 A, 2017.
- 167 C. Wongsilarat, S. Namuangruk, N. Prachumrak, T. Sudyoasak, V. Promarak, M. Sukwattanasinitt and P. Rashatasakhon, *Org. Electron.*, 2018, **57**, 352–358.
- 168 R. Grisorio, R. Iacobellis, A. Listorti, L. De Marco, M. P. Cipolla, M. Manca, A. Rizzo, A. Abate, G. Gigli and G. P. Suranna, *ACS Appl. Mater. Interfaces*, 2017, **9**, 24778–24787.
- 169 B. Wang, Q. Zeng, Z. Sun, S. Xue and M. Liang, *Dyes Pigm.*, 2019, **165**, 81–89.
- 170 C. Huang, W. Fu, C.-Z. Li, Z. Zhang, W. Qiu, M. Shi, P. Heremans, A. K. Y. Jen and H. Chen, *J. Am. Chem. Soc.*, 2016, **138**, 2528–2531.
- 171 Z. Yang, B. Xu, J. He, L. Xue, Q. Guo, H. Xia and W. Tian, *Org. Electron.*, 2009, **10**, 954–959.
- 172 H.-L. Ni, H. Monobe, P. Hu, B.-Q. Wang, Y. Shimizu and K.-Q. Zhao, *Liq. Cryst.*, 2013, **40**, 411–420.
- 173 H. Monobe, C. Chen, K. Q. Zhao, P. Hu, Y. Miyake, A. Fujii, M. Ozaki and Y. Shimizu, *Mol. Cryst. Liq. Cryst.*, 2011, **545**, 149–155.
- 174 B. Kaur, D. Moghe, A. Dey, D. Kabra and J. Jacob, *J. Lumin.*, 2018, **196**, 511–519.
- 175 L. Ma, Z. Wu, G. Zhou, F. Yuan, Y. Yu, C. Yao, S. Ning, X. Hou, Y. Li, S. Wang and Q. Gong, *J. Mater. Chem. C*, 2015, **3**, 7004–7013.
- 176 L. Sánchez, N. Martín, E. González-Cantalapiedra, A. M. Echavarren, G. M. Aminur Rahman and D. M. Guldi, *Org. Lett.*, 2006, **8**, 2451–2454.
- 177 F. Tang, K. Wu, Z. Zhou, G. Wang, Y. Pei, B. Zhao and S. Tan, *Dyes Pigm.*, 2018, **156**, 276–284.
- 178 D. Tang, J. Wan, X. Xu, Y. W. Lee, H. Y. Woo, K. Feng and Q. Peng, *Nano Energy*, 2018, **53**, 258–269.
- 179 K. Lin, B. Xie, Z. Wang, R. Xie, Y. Huang, C. Duan, F. Huang and Y. Cao, *Org. Electron.*, 2018, **52**, 42–50.
- 180 W. Wu, G. Zhang, X. Xu, S. Wang, Y. Li and Q. Peng, *Adv. Funct. Mater.*, 2018, **28**, 1707493.
- 181 K. Li, R. Xie, W. Zhong, K. Lin, L. Ying, F. Huang and Y. Cao, *Sci. China: Chem.*, 2018, **61**, 576–583.
- 182 X. Xu, G. Zhang, L. Yu, R. Li and Q. Peng, *Adv. Mater.*, 2019, **31**, 1906045.
- 183 M.-S. Yuan, Q. Fang, Z.-Q. Liu, J.-P. Guo, H.-Y. Chen, W.-T. Yu, G. Xue and D.-S. Liu, *J. Org. Chem.*, 2006, **71**, 7858–7861.
- 184 Y. Hao, M. Liang, Z. Wang, F. Cheng, C. Wang, Z. Sun and S. Xue, *Tetrahedron*, 2013, **69**, 10573–10580.
- 185 G. Ge, P. Dai, Z. Lu, M. Liang, H. Dong, Z. Sun and S. Xue, *Dyes Pigm.*, 2016, **128**, 8–18.
- 186 M. Liang, M. Lu, Q.-L. Wang, W.-Y. Chen, H.-Y. Han, Z. Sun and S. Xue, *J. Power Sources*, 2011, **196**, 1657–1664.
- 187 M.-S. Yuan, Q. Wang, W. Wang, D.-E. Wang, J. Wang and J. Wang, *Analyst*, 2014, **139**, 1541–1549.
- 188 F. Wu, J.-L. Liu, L. T. L. Lee, T. Chen, M. Wang and L.-N. Zhu, *Chin. Chem. Lett.*, 2015, **26**, 955–962.
- 189 G. V. Baryshnikov, B. F. Minaev, V. A. Minaeva, Z. Ning and Q. Zhang, *Opt. Spectrosc.*, 2012, **112**, 168–174.
- 190 P. Dai, H. Dong, M. Liang, H. Cheng, Z. Sun and S. Xue, *ACS Sustainable Chem. Eng.*, 2017, **5**, 97–104.
- 191 Y. Hao, M. Liang, Z. Wang, L. Wang, Y. Sun, Z. Sun and S. Xue, *Phys. Chem. Chem. Phys.*, 2013, **15**, 15441–15449.
- 192 X. Zong, M. Liang, C. Fan, K. Tang, G. Li, Z. Sun and S. Xue, *J. Phys. Chem. C*, 2012, **116**, 11241–11250.
- 193 M.-S. Yuan, Z.-Q. Liu and Q. Fang, *J. Org. Chem.*, 2007, **72**, 7915–7922.
- 194 P. Sam-ang, K. Silpcharu, M. Sukwattanasinitt and P. Rashatasakhon, *J. Fluoresc.*, 2019, **29**, 417–424.
- 195 P.-C. Yang, H.-W. Wen, C.-W. Huang and Y.-N. Zhu, *RSC Adv.*, 2016, **6**, 87680–87689.
- 196 P. Sam-Ang, D. Raksasorn, M. Sukwattanasinitt and P. Rashatasakhon, *RSC Adv.*, 2014, **4**, 58077–58082.
- 197 W. Huang, E. Smarsly, J. Han, M. Bender, K. Seehafer, I. Wacker, R. R. Schröder and U. H. F. Bunz, *ACS Appl. Mater. Interfaces*, 2017, **9**, 3068–3074.
- 198 N. Earmrattana, M. Sukwattanasinitt and P. Rashatasakhon, *Dyes Pigm.*, 2012, **93**, 1428–1433.
- 199 M. Echeverri, S. Gámez-Valenzuela, R. C. González-Cano, J. Guadalupe, S. Cortijo-Campos, J. T. López Navarrete, M. Iglesias, M. C. Ruiz Delgado and B. Gómez-Lor, *Chem. Mater.*, 2019, **31**, 6971–6978.
- 200 Q. Zhao, S.-H. Li, R.-L. Chai, X. Ren and C. Zhang, *ACS Appl. Mater. Interfaces*, 2020, **12**, 7504–7509.
- 201 I. Gadwal, G. Sheng, R. L. Thankamony, Y. Liu, H. Li and Z. Lai, *ACS Appl. Mater. Interfaces*, 2018, **10**, 12295–12299.
- 202 S. Che, J. Pang, A. J. Kalin, C. Wang, X. Ji, J. Lee, D. Cole, J.-L. Li, X. Tu, Q. Zhang, H.-C. Zhou and L. Fang, *ACS Mater. Lett.*, 2020, **2**, 49–54.
- 203 Q. Zhang, Y. Sun, H. Li, K. Tang, Y. Zhong, D. Wang, Y. Guo and Y. Liu, *Research*, 2021, **2021**, 1–8.
- 204 K. Lin, Z. Wang, Z. Hu, P. Luo, X. Yang, X. Zhang, M. Rafiq, F. Huang and Y. Cao, *J. Mater. Chem. A*, 2019, **7**, 19087–19093.
- 205 A. Valverde-González, C. G. López Calixto, M. Barawi, M. Gomez-Mendoza, V. A. de la Peña O'Shea, M. Liras, B. Gómez-Lor and M. Iglesias, *ACS Appl. Energy Mater.*, 2020, **3**, 4411–4420.
- 206 V. R. Battula, H. Singh, S. Kumar, I. Bala, S. K. Pal and K. Kailasam, *ACS Catal.*, 2018, **8**, 6751–6759.



- 207 S. Gámez-Valenzuela, M. Echeverri, B. Gómez-Lor, J. I. Martínez and M. C. Ruiz Delgado, *J. Mater. Chem. C*, 2020, **8**, 15416–15425.
- 208 S. Furukawa, J. Kobayashi and T. Kawashima, *Dalton Trans.*, 2010, **39**, 9329–9336.
- 209 T. Ureshino, T. Yoshida, Y. Kuninobu and K. Takai, *J. Am. Chem. Soc.*, 2010, **132**, 14324–14326.
- 210 K. Tamao, M. Uchida, T. Izumizawa, K. Furukawa and S. Yamaguchi, *J. Am. Chem. Soc.*, 1996, **118**, 11974–11975.
- 211 N. Bergman and J. Eklund, *Tetrahedron*, 1980, **36**, 1445–1450.
- 212 J. Bergman and N. Eklund, *Tetrahedron*, 1980, **36**, 1439–1443.
- 213 P. Manini, M. d'Ischia, M. Milosa and G. Prota, *J. Org. Chem.*, 1998, **63**, 7002–7008.
- 214 P. Manini, V. Criscuolo, L. Ricciotti, A. Pezzella, M. Barra, A. Cassinese, O. Crescenzi, M. G. Maglione, P. Tassini, C. Minarini, V. Barone and M. D'Ischia, *ChemPlusChem*, 2015, **80**, 919–927.
- 215 L. Ginnari-Satriani, V. Casagrande, A. Bianco, G. Ortaggi and M. Franceschin, *Org. Biomol. Chem.*, 2009, **7**, 2513–2516.
- 216 F. Wang, X.-C. Li, W.-Y. Lai, Y. Chen, W. Huang and F. Wudl, *Org. Lett.*, 2014, **16**, 2942–2945.
- 217 T. Bura, N. Leclerc, S. Fall, P. Lévêque, T. Heiser and R. Ziessel, *Org. Lett.*, 2011, **13**, 6030–6033.
- 218 T. Bura, N. Leclerc, R. Bechara, P. Lévêque, T. Heiser and R. Ziessel, *Adv. Energy Mater.*, 2013, **3**, 1118–1124.
- 219 N. Robertson, S. Parsons, E. J. MacLean, R. A. Coxall and A. R. Mount, *J. Mater. Chem.*, 2000, **10**, 2043–2047.
- 220 B. Gómez-Lor and A. M. Echavarren, *Org. Lett.*, 2004, **6**, 2993–2996.
- 221 R. A. Valentine, A. Whyte, K. Awaga and N. Robertson, *Tetrahedron Lett.*, 2012, **53**, 657–660.
- 222 N. Toworakajohnkun, M. Sukwattanasinitt and P. Rashatasakhon, *Tetrahedron Lett.*, 2017, **58**, 4149–4152.
- 223 L. Rong, Q. Liu, Y. Shi and J. Tang, *Chem. Commun.*, 2011, **47**, 2155–2157.
- 224 A. E. Sadak, A. C. Gören, Ö. A. Bozdemir and N. Saraçoğlu, *ChemistrySelect*, 2017, **2**, 10512–10516.
- 225 Q. Huaulmé, E. Cece, A. Mirloup and R. Ziessel, *Tetrahedron Lett.*, 2014, **55**, 4953–4958.
- 226 W.-Y. Lai, Q.-Y. He, R. Zhu, Q.-Q. Chen and W. Huang, *Adv. Funct. Mater.*, 2008, **18**, 265–276.
- 227 A. Babaei, K. Rakstys, S. Guelen, V. Fallah Hamidabadi, M.-G. La-Placa, L. Martínez-Sarti, M. Sessolo, H. A. Joel, O. P. M. Gaudin, V. Schanen, M. K. Nazeeruddin and H. J. Bolink, *RSC Adv.*, 2018, **8**, 35719–35723.
- 228 B. Zhao, B. Liu, R. Q. Png, K. Zhang, K. A. Lim, J. Luo, J. Shao, P. K. H. Ho, C. Chi and J. Wu, *Chem. Mater.*, 2010, **22**, 435–449.
- 229 G.-L. Feng, W.-Y. Lai, S.-J. Ji and W. Huang, *Tetrahedron Lett.*, 2006, **47**, 7089–7092.
- 230 W.-Y. Lai, Q.-Y. He, D.-Y. Chen and W. Huang, *Chem. Lett.*, 2008, **37**, 986–987.
- 231 W.-Y. Lai, R. Zhu, Q.-L. Fan, L.-T. Hou, Y. Cao and W. Huang, *Macromolecules*, 2006, **39**, 3707–3709.
- 232 M. Sang, S. Cao, J. Yi, J. Huang, W.-Y. Lai and W. Huang, *RSC Adv.*, 2016, **6**, 6266–6275.
- 233 Z. Yao, X. Liao, Y. Guo, H. Zhao, Y. Guo, F. Zhang, L. Zhang, Z. Zhu, L. Kloo, W. Ma, Y. Chen and L. Sun, *Chem. Mater.*, 2019, **31**, 8810–8819.
- 234 B. Gómez-Lor, B. Alonso, A. Omenat and J. L. Serrano, *Chem. Commun.*, 2006, 5012–5014.
- 235 E. M. García-Frutos and B. Gómez-Lor, *Organic Field-Effect Transistors VIII*, Proc. of SPIE, 2009, vol. 7417, pp. 74170J1.
- 236 J. Luo, B. Zhao, J. Shao, K. A. Lim, H. S. On Chan and C. Chi, *J. Mater. Chem.*, 2009, **19**, 8327–8334.
- 237 Y.-C. Hu, Z.-L. Lin, T.-C. Huang, J.-W. Lee, W.-C. Wei, T.-Y. Ko, C.-Y. Lo, D.-G. Chen, P.-T. Chou, W.-Y. Hung and K.-T. Wong, *Mater. Chem. Front.*, 2020, **4**, 2029–2039.
- 238 S. Zhang, W. Chen, G. Dai, F. Yang and L. Chen, *Asian J. Org. Chem.*, 2018, **7**, 2223–2227.
- 239 B. Gómez-Lor, G. Hennrich, B. Alonso, M. Á. Monge, E. Gutiérrez-Puebla and A. M. Echavarren, *Angew. Chem., Int. Ed.*, 2006, **45**, 4491–4494.
- 240 E. M. García-Frutos, B. Gómez-Lor, M. Á. Monge, E. Gutiérrez-Puebla, I. Alkorta and J. Elguero, *Chem. – Eur. J.*, 2008, **14**, 8555–8561.
- 241 Y. Chen, X. Wu, Y. Liu, L. Chen, H. Li, W. Wang, S. Wang, H. Tian, H. Tong and L. Wang, *J. Mater. Chem. C*, 2019, **7**, 7900–7905.
- 242 G. Otero, G. Biddau, C. Sánchez-Sánchez, R. Caillard, M. F. López, C. Rogero, F. J. Palomares, N. Cabello, M. A. Basanta, J. Ortega, J. Méndez, A. M. Echavarren, R. Pérez, B. Gómez-Lor and J. A. Martín-Gago, *Nature*, 2008, **454**, 865–868.
- 243 C. Ruiz, E. M. García-Frutos, D. A. da Silva Filho, J. T. López Navarrete, M. C. Ruiz Delgado and B. Gómez-Lor, *J. Phys. Chem. C*, 2014, **118**, 5470–5477.
- 244 E. M. García-Frutos, E. Gutierrez-Puebla, M. A. Monge, R. Ramírez, P. de Andrés, A. de Andrés, R. Ramírez and B. Gómez-Lor, *Org. Electron.*, 2009, **10**, 643–652.
- 245 F. Gallego-Gómez, E. M. García-Frutos, J. M. Villalvilla, J. A. Quintana, E. Gutiérrez-Puebla, M. Á. Monge, M. A. Díaz-García and B. Gómez-Lor, *Adv. Funct. Mater.*, 2011, **21**, 738–745.
- 246 T. Han, I. Bulut, S. Méry, B. Heinrich, P. Lévêque, N. Leclerc and T. Heiser, *J. Mater. Chem. C*, 2017, **5**, 10794–10800.
- 247 A. Benito-Hernández, U. K. Pandey, E. Cavero, R. Termine, E. M. García-Frutos, J. L. Serrano, A. Golemme and B. Gómez-Lor, *Chem. Mater.*, 2013, **25**, 117–121.
- 248 Z. Li, S. Liu, Q. Zhang and D. Liu, *Integr. Ferroelectr.*, 2013, **144**, 112–117.
- 249 F. Zhao, C. Liu, Y. Sun, Q. Li, J. Zhao, Z. Li, B. Zhang, C. Lu, Q. Li, S. Qiao and Y. S. Zhao, *Org. Electron.*, 2019, **74**, 276–281.
- 250 M. Reig, J. Puigdollers and D. Velasco, *J. Mater. Chem. C*, 2015, **3**, 506–513.
- 251 M. Reig, G. Bagdziunas, A. Ramanavicius, J. Puigdollers and D. Velasco, *Phys. Chem. Chem. Phys.*, 2018, **20**, 17889–17898.



- 252 C. Li, Y. Wang, Y. Zou, X. Zhang, H. Dong and W. Hu, *Angew. Chem., Int. Ed.*, 2020, **59**, 9403–9407.
- 253 S. W. Shelton, T. L. Chen, D. E. Barclay and B. Ma, *ACS Appl. Mater. Interfaces*, 2012, **4**, 2534–2540.
- 254 C. Kulshreshtha, G. W. Kim, R. Lampande, D. H. Huh, M. Chae and J. H. Kwon, *J. Mater. Chem. A*, 2013, **1**, 4077–4082.
- 255 F. Zhang, X. Yang, M. Cheng, J. Li, W. Wang, H. Wang and L. Sun, *J. Mater. Chem. A*, 2015, **3**, 24272–24280.
- 256 L. Calió, C. Momblona, L. Gil-Escrig, S. Kazim, M. Sessolo, Á. Sastre-Santos, H. J. Bolink and S. Ahmad, *Sol. Energy Mater. Sol. Cells*, 2017, **163**, 237–241.
- 257 D. R. Kil, C. Lu, J.-M. Ji, C. H. Kim and H. K. Kim, *Nanomaterials*, 2020, **10**, 936.
- 258 T. Techajaronjit, S. Namuangruk, N. Prachumrak, V. Promarak, M. Sukwattanasinitt and P. Rashatasakhon, *RSC Adv.*, 2016, **6**, 56392–56398.
- 259 Q. Ye, J. Chang, J. Shao and C. Chi, *J. Mater. Chem.*, 2012, **22**, 13180.
- 260 L. A. Illicachi, J. Urieta-Mora, J. Calbo, J. Aragón, C. Igei, I. García-Benito, C. Momblona, B. Insuasty, A. Ortiz, C. Roldán-Carmona, A. Molina-Ontoria, E. Ortí, N. Martín and M. K. Nazeeruddin, *Chem. – Eur. J.*, 2020, **26**, 11039–11047.
- 261 F. J. Ramos, K. Rakstys, S. Kazim, M. Grätzel, M. K. Nazeeruddin and S. Ahmad, *RSC Adv.*, 2015, **5**, 53426–53432.
- 262 K. Rakstys, A. Abate, M. I. Dar, P. Gao, V. Jankauskas, G. Jacopin, E. Kamarauskas, S. Kazim, S. Ahmad, M. Grätzel and M. K. Nazeeruddin, *J. Am. Chem. Soc.*, 2015, **137**, 16172–16178.
- 263 I. Petrikyte, I. Zimmermann, K. Rakstys, M. Daskeviciene, T. Malinauskas, V. Jankauskas, V. Getautis and M. K. Nazeeruddin, *Nanoscale*, 2016, **8**, 8530–8535.
- 264 A. Connell, Z. Wang, Y.-H. Lin, P. C. Greenwood, A. A. Wiles, E. W. Jones, L. Furnell, R. Anthony, C. P. Kershaw, G. Cooke, H. J. Snaith and P. J. Holliman, *J. Mater. Chem. C*, 2019, **7**, 5235–5243.
- 265 P.-Y. Su, L.-B. Huang, J.-M. Liu, Y.-F. Chen, L.-M. Xiao, D.-B. Kuang, M. Mayor and C.-Y. Su, *J. Mater. Chem. A*, 2017, **5**, 1913–1918.
- 266 L. Shen, X. Yang, J. An, L. Zhang, K. Yang and Z. Deng, *ChemistrySelect*, 2021, **6**, 4645–4650.
- 267 X. Qian, Y.-Z. Zhu, J. Song, X.-P. Gao and J.-Y. Zheng, *Org. Lett.*, 2013, **15**, 6034–6037.
- 268 X. Qian, L. Lu, Y.-Z. Zhu, H.-H. Gao and J.-Y. Zheng, *Dyes Pigm.*, 2015, **113**, 737–742.
- 269 P. Qin, P. Sanghyun, M. I. Dar, K. Rakstys, H. ElBatal, S. A. Al-Muhtaseb, C. Ludwig and M. K. Nazeeruddin, *Adv. Funct. Mater.*, 2016, **26**, 5550–5559.
- 270 K. Rakstys, S. Paek, P. Gao, P. Gratia, T. Marszalek, G. Grancini, K. T. Cho, K. Genevicius, V. Jankauskas, W. Pisula and M. K. Nazeeruddin, *J. Mater. Chem. A*, 2017, **5**, 7811–7815.
- 271 R. R. Reghu, D. Volyniuk, N. Kostiv, K. Norvaisa and J. V. Grazulevicius, *Dyes Pigm.*, 2016, **125**, 159–168.
- 272 Z.-L. Zhang, L.-Y. Zou, A.-M. Ren, Y.-F. Liu, J.-K. Feng and C.-C. Sun, *Dyes Pigm.*, 2013, **96**, 349–363.
- 273 Y. Liu, X. Wu, Y. Chen, L. Chen, H. Li, W. Wang, S. Wang, H. Tian, H. Tong and L. Wang, *J. Mater. Chem. C*, 2019, **7**, 9719–9725.
- 274 Y. Chen, S. Wang, X. Wu, Y. Xu, H. Li, Y. Liu, H. Tong and L. Wang, *J. Mater. Chem. C*, 2018, **6**, 12503–12508.
- 275 K. J. Kim, G. H. Kim, R. Lampande, D. H. Ahn, J. B. Im, J. S. Moon, J. K. Lee, J. Y. Lee, J. Y. Lee and J. H. Kwon, *J. Mater. Chem. C*, 2018, **6**, 1343–1348.
- 276 S. J. Yoon, J. H. Kim, W. J. Chung and Y. J. Lee, *Chem. – Eur. J.*, 2021, **27**, 3065–3073.
- 277 J. Eng, J. Hagon and T. J. Penfold, *J. Mater. Chem. C*, 2019, **7**, 12942–12952.
- 278 L. Ji, Q. Fang, M.-S. Yuan, Z.-Q. Liu, Y.-X. Shen and H.-F. Chen, *Org. Lett.*, 2010, **12**, 5192–5195.
- 279 J. Zhang, L. Gong, X. Zhang, M. Zhu, C. Su, Q. Ma, D. Qi, Y. Bian, H. Du and J. Jiang, *Chem. – Eur. J.*, 2020, **26**, 13842–13848.
- 280 Y.-F. Xie, S.-Y. Ding, J.-M. Liu, W. Wang and Q.-Y. Zheng, *J. Mater. Chem. C*, 2015, **3**, 10066–10069.
- 281 A. Alkaş, J. Cornelio and S. G. Telfer, *Chem. – Asian J.*, 2018, **14**, 1167–1174.
- 282 A. Alkas and S. G. Telfer, *Aust. J. Chem.*, 2019, **72**, 786–796.
- 283 W. Lai, D. Liu and W. Huang, *Sci. China: Chem.*, 2010, **53**, 2472–2480.
- 284 X.-C. Li, Y. Zhang, C.-Y. Wang, Y. Wan, W.-Y. Lai, H. Pang and W. Huang, *Chem. Sci.*, 2017, **8**, 2959–2965.
- 285 A. E. Sadak, E. Karakuş, Y. M. Chumakov, N. A. Dogan and C. T. Yavuz, *ACS Appl. Energy Mater.*, 2020, **3**, 4983–4994.
- 286 Y. Xu, X. Wu, Y. Chen, H. Hang, H. Tong and L. Wang, *RSC Adv.*, 2016, **6**, 31915–31918.
- 287 Y. Xu, X. Wu, Y. Chen, H. Hang, H. Tong and L. Wang, *Polym. Chem.*, 2016, **7**, 4542–4548.
- 288 X. Li, C. Wang, W. Song, C. Meng, C. Zuo, Y. Xue, W. Lai and W. Huang, *ChemPlusChem*, 2019, **84**, 1623–1629.
- 289 X.-C. Li, C.-Y. Wang, Y. Wan, W.-Y. Lai, L. Zhao, M.-F. Yin and W. Huang, *Chem. Commun.*, 2016, **52**, 2748–2751.
- 290 Y. Xu, H. Li, X. Wu, Y. Chen, H. Hang, H. Tong and L. Wang, *Polym. Chem.*, 2017, **8**, 2484–2489.
- 291 E. Andrikaityte, J. Simokaitiene, A. Tomkeviciene, J. V. Grazulevicius and V. Jankauskas, *Mol. Cryst. Liq. Cryst.*, 2014, **590**, 121–129.
- 292 N. Li, Y. Chen, S. Duan, G. Chen, Y. Xu, H. Tong, Y. Sanehira, T. Miyasaka, A. Li and X.-F. Wang, *J. Photochem. Photobiol., A*, 2020, **389**, 112228.
- 293 G. Hu, S. P. Kitney, S. M. Kelly, W. Harrison, B. Lambert and M. O'Neill, *RSC Adv.*, 2018, **8**, 8580–8585.
- 294 Q. Wang, R. Li, X. Ouyang and G. Wang, *RSC Adv.*, 2019, **9**, 40531–40535.
- 295 D. Zhang, T. K. Ronson, J. L. Greenfield, T. Brotin, P. Berthault, E. Léonce, J.-L. Zhu, L. Xu and J. R. Nitschke, *J. Am. Chem. Soc.*, 2019, **141**, 8339–8345.
- 296 D. Zhang, T. K. Ronson, S. Güryel, J. D. Thoburn, D. J. Wales and J. R. Nitschke, *J. Am. Chem. Soc.*, 2019, **141**, 14534–14538.



- 297 A. E. Sadak and E. Karakuş, *J. Fluoresc.*, 2020, **30**, 213–220.
- 298 N. N. Ghosh, M. Habib, A. Pramanik, P. Sarkar and S. Pal, *New J. Chem.*, 2019, **43**, 6480–6491.
- 299 K.-R. Wang, H.-W. An, D. Han, F. Qian and X.-L. Li, *Chin. Chem. Lett.*, 2013, **24**, 467–470.
- 300 M. Franceschin, L. Ginnari-Satriani, A. Alvino, G. Ortaggi and A. Bianco, *Eur. J. Org. Chem.*, 2010, 134–141.
- 301 A. Cummaro, I. Fotticchia, M. Franceschin, C. Giancola and L. Petraccone, *Biochimie*, 2011, **93**, 1392–1400.
- 302 L. Petraccone, I. Fotticchia, A. Cummaro, B. Pagano, L. Ginnari-Satriani, S. Haider, A. Randazzo, E. Novellino, S. Neidle and C. Giancola, *Biochimie*, 2011, **93**, 1318–1327.
- 303 T. Kojima, S. Furukawa, H. Tsuji and E. Nakamura, *Chem. Lett.*, 2014, **43**, 676–677.
- 304 D. Christian, T. H. Nguyen, M. Lonka and M. Jacques, *Mol. Cryst. Liq. Cryst.*, 1984, **114**, 139–150.
- 305 J. Bergman and B. Egestad, *Chem. Scr.*, 1986, **26**, 287–292.
- 306 *JP* 08146221 A, 1996.
- 307 *JP* 10324661 A, 1998.
- 308 H. Kaida, T. Satoh, Y. Nishii, K. Hirano and M. Miura, *Chem. Lett.*, 2016, **45**, 1069–1071.
- 309 S. Nakamura, M. Okamoto, N. Tohnai, K. Nakayama, Y. Nishii and M. Miura, *Bull. Chem. Soc. Jpn.*, 2020, **93**, 99–108.
- 310 *JP* 11092427 A, 1999, 1–17.
- 311 T. H. Nguyen, R. Cayuela, C. Destrade and J. Malthete, *Mol. Cryst. Liq. Cryst.*, 1985, **122**, 141–149.
- 312 J. Bergman and B. Egestad, *Tetrahedron*, 1986, **42**, 763–773.
- 313 R. Cayuela, T. H. Nguyen, C. Destrade and A. M. Levelut, *Mol. Cryst. Liq. Cryst.*, 1989, **177**, 81–91.
- 314 *US* 5637669 A, 1997.
- 315 *KR* 20140000611 A, 2014.
- 316 *WO* 2014111400 7A1, 2014.
- 317 *KR* 20110005476 A, 2011.
- 318 *US* 2016/0233427 A1, 2016.
- 319 Q. Xiao, T. Sakurai, T. Fukino, K. Akaike, Y. Honsho, A. Saeki, S. Seki, K. Kato, M. Takata and T. Aida, *J. Am. Chem. Soc.*, 2013, **135**, 18268–18271.
- 320 S. Limberti, L. Emmett, A. Trandafir, G. Kociok-Köhn and G. D. Pantoş, *Chem. Sci.*, 2019, **10**, 9565–9570.
- 321 K. Górski, J. Mech-Piskorz, K. Noworyta, B. Leśniewska and M. Pietraszkiewicz, *New J. Chem.*, 2018, **42**, 5844–5852.
- 322 K. Górski, J. Mech-Piskorz, B. Leśniewska, O. Pietraszkiewicz and M. Pietraszkiewicz, *J. Org. Chem.*, 2019, **84**, 11553–11561.
- 323 M. R. Maciejczyk, J. A. G. Williams, N. Robertson and M. Pietraszkiewicz, *RSC Adv.*, 2017, **7**, 49532–49535.
- 324 K. Górski, J. Mech-Piskorz, B. Leśniewska, O. Pietraszkiewicz and M. Pietraszkiewicz, *J. Org. Chem.*, 2020, **85**, 4672–4681.
- 325 M. T. El Sayed, L. Wessjohann, A. Porzel and A. Hilgeroth, *J. Heterocycl. Chem.*, 2016, **54**, 1077–1083.
- 326 A. Benito-Hernández, M. T. El Sayed, J. T. López Navarrete, M. C. Ruiz Delgado and B. Gómez-Lor, *Org. Chem. Front.*, 2018, **5**, 1748–1755.
- 327 M. T. El Sayed, S. N. Shabaan, A. E. Sarhan, S. M. El-Messery, S. M. El-Sayed and G. S. Hassan, *Bioorg. Chem.*, 2020, **104**, 104323.
- 328 K. Kobayashi, N. Suzue, R. Ishii, R. Kamiya and H. Wakabayashi, *Heterocycles*, 2009, **78**, 2467–2475.

